A&A 485, 315–325 (2008)
DOI: 10.1051/0004-6361:20078255

Astronomy & Astrophysics

Nonlinear cooling of relativistic particles under equipartition conditions

II. Instantaneous power law injection⋆

R. Schlickeiser and I. Lerche

Institut für Theoretische Physik, Lehrstuhl IV: Weltraum- und Astrophysik, Ruhr-Universität Bochum, 44780 Bochum, Germany
e-mail: rsch@tp4.rub.de

Received 11 July 2007 / Accepted 20 March 2008

ABSTRACT

Aims. In powerful cosmic nonthermal radiation sources with dominant magnetic-field self generation, the plasma physical processes generating these magnetic fields by relativistic plasma instabilities are closely related to the processes energising ultra-high energy radiating electrons in these sources. Then the magnetic field strength becomes time-dependent and adjusts itself to the actual kinetic energy density of the radiating electrons. As a consequence, the synchrotron radiation cooling of individual relativistic electrons exhibits a nonlinear behaviour because of the dependence of the magnetic energy density on the actual time-varying kinetic energy density.
Methods. The nonlinear kinetic equation for the intrinsic temperoral evolution of relativistic electrons is solved for the case of instantaneous injection of power-law distributed electrons.
Results. The properties of the resulting approximate, nonlinear electron density show significant differences compared to the standard linear solution for constant non-equipartition magnetic-field energy density as, for instance, the different time behaviour of the upper and lower cut-offs of the electron distribution. Also the differential electron fluence as a function of electron energy differs from the linear fluence. For large spectral indices $s > 2$ of the injected power law, the nonlinear fluence exhibits a weaker break at the lower injected electron cut-off γ_1 than the linear fluence. For small spectral indices $1 < s < 2$, the nonlinear fluence shows no break at all and approaches a $\propto\gamma^{-3}$ power law at all energies below $\gamma_2/2$.
Conclusions. For electron radiation processes not subject to equipartition conditions, such as inverse Compton scattering of ambient photon gases and relativistic bremsstrahlung, the energy dependences of the electron number density and the electron fluence can be directly used to infer the frequency dependence of the fluxes and fluences of the generated photons. For steep (spectral index $s > 2$) injected power laws, the nonlinear synchrotron fluence at low frequencies approaches a power law $\propto\nu^{-0.6}$, independent of the value of s, which is identical to the synchrotron fluence behaviour from monoenergetically injected relativistic electrons.

Key words. galaxies: active – radiation mechanisms: non-thermal – ISM: cosmic rays

1. Introduction

Simplified homogenous one-zone models for the relativistically moving emission regions in the jets of active galactic nuclei and gamma-ray burst afterglows are remarkably successful in quantitatively reproducing the observed broadband nonthermal photon spectra. In the standard model for blazars, nonthermal synchrotron emission is radiated by electrons accelerated by Fermi-type processes to ultrarelativistic Lorentz factors. These electrons also Compton-scatter all ambient radiation fields, including the internal synchrotron field (Maraschi et al. 1992; Bloom & Marscher 1996; Tavecchio et al. 1998) and the external radiation fields traversed by the jet (Melia & Königl 1989; Dermer & Schlickeiser 1993; Sikora et al. 1994; Arbeiter et al. 2005). The intensities of the individual radiation components depend on the properties of the radiation fields, the properties of the relativistic outflows, and the time-dependent spectral injection of electrons into the outflow. The evolving energy distribution of the radiating electrons is obtained by solving a continuity kinetic equation balancing the competition of injection, escape, and energy loss processes. The numerical modelling of the observed spectral energy distributions (Dermer & Schlickeiser 2002; Böttcher & Chiang 2002) provides the best agreement if equipartition conditions are taken between the energy densities of magnetic fields ($U_B = B^2/8\pi$) and relativistic electrons $U_e(t) = \int_0^\infty \mathrm{d}p\gamma m_e c^2 N(p,t)$.

Similar equipartition arguments have been made in the nonthermal radiation models for gamma-ray burst afterglows (Meszaros & Rees 1993, 1997; Paczynski & Rhoads 1993; Frail et al. 2000). The cosmological fireball model adopts a spherical blast wave expanding adiabatically into a homogeneous medium. It is assumed that a fixed fraction ϵ_e of the blast-wave energy E_0 goes into accelerating a power law distribution of electrons above a lower ultrarelativistic cut-off γ_m. In the presence of a magnetic field, which itself is a fixed fraction ϵ_B of the energy density of the blast wave, the electrons emit synchrotron radiation. The ratio ϵ_B/ϵ_e of the fixed fractions thus reflects the equipartition condition in the emission region (Sari et al. 1998; Frail et al. 2000; Van der Horst et al. 2008).

Recently we have noted (Schlickeiser & Lerche 2007 – hereinafter referred to as SL) that this generation of magnetic fields at almost equipartition strength by relativistic plasma instabilities operates as fast as the acceleration or injection of ultra-high energy radiating electrons in these sources (especially in powerful

⋆ Appendices A–C are only available in electronic form at http://www.aanda.org

nonthermal radiation sources). At least initially, the magnetic field strength then becomes time-dependent and adjusts to the actual kinetic energy density of the radiating electrons in these sources. Here we assume that the magnetic field strength is tied by a fixed partition ratio e_B to the kinetic energy density of the radiating relativistic electrons. As the relativistic particles cool by their radiative synchrotron losses, the magnetic field will decay accordingly. Although there is no obvious physical justification for this partition behaviour, the success of the radiation modelling of jets of active galactic nuclei and gamma-ray burst afterglows with incorporated partition behaviour justifies exploring the physical consequences of this observational finding.

The coupling of the magnetic field energy density to the energy of the radiating particles changes both the synchrotron emissivity and the intrinsic temporal evolution of the relativistic electron energy spectrum after injection. Nonlinear cooling of electrons is potentially important in flaring high-energy blazar sources, such as PKS 2155-304 (Aharonian et al. 2007), because it allows an observational distinction of time-dependent electron photon emissivities (by synchrotron and inverse Compton emission) against hadronic photon emissivities (from neutral pion decay). As discussed in Schlickeiser (2008), the observed TeV fluence spectrum from the 29–30 July outburst of PKS 2155-304 is reproduced rather well by the synchrotron self-Compton radiation from nonlinearly cooling relativistic electrons. Synchrotron losses of hadrons are negligibly small so that hadrons and their radiation products will not exhibit the nonlinear cooling behaviour.

SL illustrated the nonlinear cooling effect and its differences to the linear cooling behaviour for the case of instantaneous injection of monoenergetic ultrarelativistic electrons. Here we consider the case of instantaneous injection of power-law distributed electrons into a physical system where equipartition conditions hold between the energy densities of magnetic fields ($U_B = B^2/8\pi$) and relativistic electrons,

$$U_e(t) = \int_0^\infty dp \gamma m_e c^2 N(p,t), \tag{1}$$

i.e. constant values of the equipartition parameter $e_B = U_B(t)/U_e(t)$. Consequently, the magnetic field strength becomes time-dependent

$$B(t) = \sqrt{8\pi e_B U_e(t)}, \tag{2}$$

adjusting to the actual kinetic energy density of the radiating particles. The consequences are twofold:

(1) because the magnetic field strength (2) is time-dependent, the synchrotron photon emissivity and fluence will be modified as compared to the standard constant magnetic field case;
(2) the synchrotron radiation cooling of individual relativistic electrons exhibits a nonlinear behaviour because the magnetic energy density $U_B(t)$ entering the synchrotron energy-loss rate now depends on the kinetic energy density of the radiating particles, which, according to Eq. (1), is an integral over the electron differential spectral density.

After identifying the basic equations we highlight the differences of the electron equilibrium energy spectra by solving the time-dependent volume-averaged kinetic equations under linear (U_B = const. and B = const.) and nonlinear ($U_B(t)$ and $B(t)$) equipartition conditions, respectively. In each case we calculate the differences in the produced time-dependent synchrotron radiation spectra and synchrotron fluences.

2. Basic kinetic equation

All physical quantities are calculated in a coordinate system comoving with the radiation source. The energy loss rate of relativistic electrons due to synchrotron radiation in a large-scale random magnetic field is

$$|\dot{\gamma}| = \frac{4}{3}\frac{c\sigma_T}{m_e c^2} U_B \gamma^2 \tag{3}$$

where γ is the electron Lorentz factor, c denotes the speed of light, and $\sigma_T = 6.65 \times 10^{-25}$ cm^2 is the Thomson cross-section.

We consider the instantaneous injection of power-law distributed ultrarelativistic electrons at the rate

$$Q(\gamma,t) = q_0 \gamma^{-s} \delta(t), \quad 1 \ll \gamma_1 \le \gamma \le \gamma_2 \tag{4}$$

at time $t = 0$ with a constant value of the power-law spectral index s. The competition between this instantaneous injection rate and the electron synchrotron energy losses is described by the time-dependent kinetic equation for the volume-averaged relativistic electron population inside the radiating source (Kardashev 1962):

$$\frac{\partial n(\gamma,t)}{\partial t} - \frac{\partial}{\partial \gamma}\left[|\dot{\gamma}|\, n(\gamma,t)\right] = Q(\gamma,t) \tag{5}$$

where $n(\gamma,t)$ is the volume-averaged differential number density. Throughout, we consider ultrarelativistic electrons ($\gamma \gg 1$) so that the relation $p \simeq m_e c\gamma$ is appropriate, implying the relation $N(p,t) = n(\gamma,t)/m_e c$ between the respective differential electron densities. The kinetic energy density in relativistic electrons then is $U_e(t) = m_e c^2 \int_0^\infty d\gamma \gamma n(\gamma,t)$. When illustrating our results in the following, we use as variable the normalised Lorentz factor

$$g \equiv \gamma/\gamma_1, \tag{6}$$

where γ_1 denotes the initial lower cut-off in the power-law injection rate (4), and the notation

$$g_2 = \gamma_2/\gamma_1. \tag{7}$$

3. Linear cooling solution

In the case of *linear* cooling with constant energy density U_B we can use Eq. (SL-6) as the Green's function to obtain the solution of the kinetic Eq. (5) as

$$n_L(\gamma,t) = q_0 \gamma^{-s}[1 - D_0\gamma t]^{s-2} H[t] H\left[\gamma - \frac{\gamma_1}{1 + D_0\gamma_1 t}\right] \times H\left[\frac{\gamma_2}{1 + D_0\gamma_2 t} - \gamma\right], \tag{8}$$

where $H[x]$ denotes Heaviside's step function and with the constant rate

$$D_0 = \frac{4}{3}\frac{c\sigma_T}{m_e c^2} U_B = 2.66 \times 10^{-14}\left[\frac{U_B}{m_e c^2}\right] \mathrm{s}^{-1}. \tag{9}$$

The solution (8) is well known (Kardashev 1962) and exhibits the Kardashev pile-up for flat ($s < 2$) injected power laws. In Fig. 1 we illustrate the time dependence of the linear electron distribution at different times after injection for $s = 1.5$. The electrons pile up at a maximum Lorentz factor that decreases with time. Moreover the initially broad power-law distribution is significatly quenched with increasing time.

Figure 2 shows the time dependence of the linear electron distribution for $s = 3$. Here the power law appears between sharp

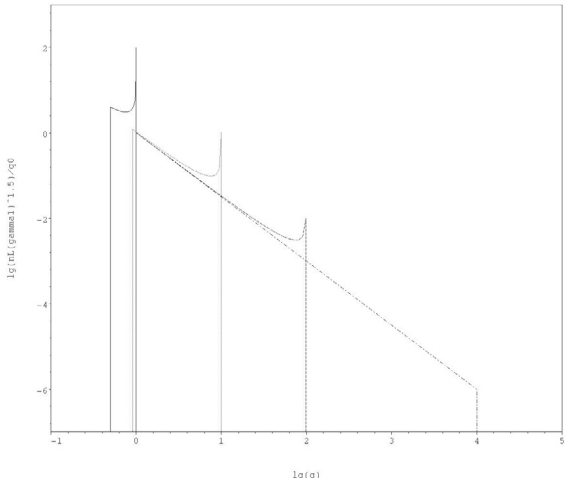

Fig. 1. Electron distribution function $n_L\gamma_1^{3/2}/q_0$ as a function of the normalised Lorentz factor $g = \gamma/\gamma_1$ for $s = 1.5$ and $g_2 = \gamma_2/\gamma_1 = 10^4$ in the linear cooling case at different times $\tau = t/t_M = 0$ (dotted-dashed curve), 10^{-2} (dashed curve), 0.1 (thin full curve), and 1 (thick full curve). Here $t_M = D_0\gamma_1$.

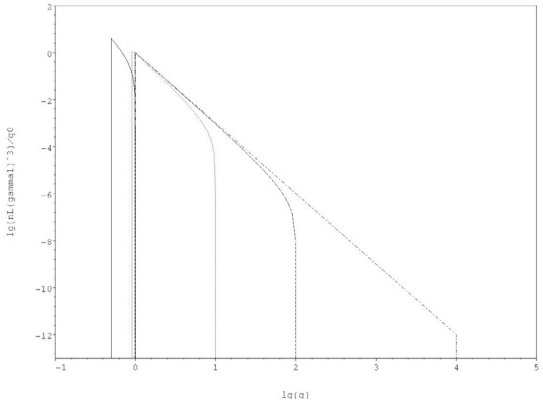

Fig. 2. Electron distribution function $n_L\gamma_1^3/q_0$ as a function of the normalised Lorentz factor $g = \gamma/\gamma_1$ for $s = 3$ and $g_2 = \gamma_2/\gamma_1 = 10^4$ in the linear cooling case at different times $\tau = t/t_M = 0$ (dotted-dashed curve), 10^{-2} (dashed curve), 0.1 (thin full curve), and 1 (thick full curve). Here $t_M = D_0\gamma_1$.

lower and upper cutoffs that decrease with time. One also notices the significant quenching of the power law with increasing time.

For the linear cooling case, solution (8) serves as Green's function, which allowed Kardashev (1962) to derive solutions of the electron kinetic equation for any energy dependence of the injection rate by simple quadratures in just one paper. This comfortable situation does not apply to the solution of the nonlinear electron kinetic equation. Because of the nonlinearity of the kinetic equation the Green's function method does not apply, and one has to derive each solution separately for different energy dependences of the injection rate.

4. Nonlinear cooling solution

In the nonlinear case the magnetic field energy density

$$U_B(t) = e_B U_e(t) = e_B m_e c^2 \int_0^\infty d\gamma\gamma n(\gamma, t)$$

depends on an energy integral of the actual electron spectrum, so that the loss rate (3) is

$$|\dot{\gamma}| = A_0\gamma^2 \int_0^\infty d\gamma\gamma n(\gamma, t) \tag{10}$$

with the abbreviation $A_0 = \frac{4}{3}c\sigma_T e_B$ cm^3 s^{-1}. In this case the solution of the *nonlinear* kinetic equation is (Appendix A)

$$n(\gamma, y \geq 0) = \frac{q_0}{\gamma^2}\left(\gamma^{-1} - T(y)\right)^{s-2} H[x - T(y) - x_2]$$

$$\times H[x_1 + T(y) - x]\,(1 - H[T(y) - x])$$

$$= q_0\gamma^{-s}(1 - \gamma T(y))^{s-2} H\left[\frac{\gamma_2}{1 + \gamma_2 T(y)} - \gamma\right]$$

$$\times H\left[\gamma - \frac{\gamma_1}{1 + \gamma_1 T(y)}\right] H\left[\frac{1}{T(y)} - \gamma\right] \tag{11}$$

where the variable $T(y)$ is related to the time variable $y = A_0 t$ through the first-order nonlinear differential equation

$$T^{2-s}\frac{dT}{dy} = q_0 \int_{x_2/T}^{x_1/T} dv \frac{v^{s-2}}{v + 1}\cdot \tag{12}$$

As shown in Appendix B, the nonlinear differential Eq. (12) can be solved approximately in the small time ($T \leq x_2 \ll x_1$), the intermediate time ($x_2 \leq T \leq x_1$), and the late time ($x_2 \ll x_1 \leq T$) limits, respectively.

For flat spectral index values $1 < s < 2$, we obtain approximately

$$T(0 \leq y \leq y_2, s < 2) \simeq \frac{q_0}{2 - s} x_2^{s-2} y,$$

$$T(y_2 \leq y \leq y_1, s < 2) \simeq \left[\frac{3 - s}{(2 - s)(s - 1)} q_0 y - \frac{2(2 - s)}{s - 1} x_2^{3-s}\right]^{1/(3-s)},$$

$$T(y \geq y_1) \simeq \left[\frac{2q_0}{s-1} x_1^{s-1} y + \frac{s-1}{3-s} x_1^2 - \frac{4(2-s)^2}{(3 - s)(s - 1)} x_2^{3-s} x_1^{s-1}\right]^{1/2} \tag{13}$$

with

$$y_1 = \frac{(2 - s)(s - 1)}{(3 - s)q_0}\left[x_1^{3-s} + \frac{2(2 - s)}{s - 1} x_2^{3-s}\right] \tag{14}$$

and

$$y_2 = \frac{2 - s}{q_0} x_2^{3-s}. \tag{15}$$

For steep spectral index values $s > 2$, we find approximately

$$T(y, s > 2) \simeq \begin{cases} \frac{q_0}{s-2} x_1^{s-2} y & \text{for } 0 \leq y \leq \frac{s-2}{q_0} x_1^{3-s} \\ \left[\frac{2q_0}{s-1} x_1^{s-1} y + \frac{3-s}{s-1} x_1^2\right]^{1/2} & \text{for } y \geq \frac{s-2}{q_0} x_1^{3-s}. \end{cases} \tag{16}$$

Both approximations can be used in Eq. (11).

4.1. Steep injection power laws $s > 2$

For a steep spectral index value $s > 2$, introduce the time scale

$$t_{\rm L} \equiv \frac{s-2}{q_0 A_0 \gamma_1^{3-s}}, \tag{17}$$

which is inversely proportional to the particle injection rate q_0. This is easy to understand: as the rate of nonlinear cooling depends on the energy density of relativistic particles, the nonlinear cooling time scales depend on the parameters of the injected energy density of particles $U_{\rm e}(0) = m_{\rm e}c^2 K$ with

$$\begin{aligned} K &= \int_{\gamma_1}^{\gamma_2} {\rm d}\gamma \gamma q_0 \gamma^{-s} = \frac{q_0}{2-s}\left[\gamma_2^{2-s} - \gamma_1^{2-s}\right] \\ &\simeq q_0 \begin{cases} \frac{\gamma_2^{2-s}}{2-s} & \text{for } s < 2 \\ \frac{\gamma_1^{2-s}}{s-2} & \text{for } s > 2. \end{cases} \end{aligned} \tag{18}$$

For the steep ($s > 2$) power laws considered here, the injected energy density K is determined by the lower cut-off γ_1 of the particles. With Eq. (18), the time scale (17) simply reads

$$t_{\rm L} = (A_0 \gamma_1 K)^{-1}. \tag{19}$$

The solution to the nonlinear kinetic equation then is approximately

$$n(\gamma, 0 \le t \le t_{\rm L}, s > 2) \simeq q_0 \gamma^{-s}\left[1 - \frac{\gamma}{\gamma_1}\frac{t}{t_{\rm L}}\right]^{s-2} \times H\left[\frac{\gamma_2}{1+\frac{\gamma_2}{\gamma_1}\frac{t}{t_{\rm L}}} - \gamma\right] H\left[\gamma - \frac{\gamma_1}{1+\frac{t}{t_{\rm L}}}\right] H\left[\gamma_1 \frac{t_{\rm L}}{t} - \gamma\right] \tag{20}$$

and

$$n(\gamma, t \ge t_{\rm L}, s > 2) \simeq q_0 \gamma^{-s}\left[1 - \frac{\gamma}{\gamma_1}A(t)\right]^{s-2} \times H\left[\frac{\gamma_2}{1+\frac{\gamma_2}{\gamma_1}A(t)} - \gamma\right] H\left[\gamma - \frac{\gamma_1}{1+A(t)}\right] H\left[\frac{\gamma_1}{A(t)} - \gamma\right] \tag{21}$$

with

$$A(t) = \sqrt{\frac{2(s-2)}{s-1}\frac{t}{t_{\rm L}} + \frac{3-s}{s-1}}. \tag{22}$$

Both solutions agree at $t = t_{\rm L}$.

4.2. Flat injection power laws $1 < s < 2$

For low spectral index values, the short time behaviour of the approximate solution to the nonlinear kinetic equation is more involved. Introduce the two time scales

$$t_{\rm M} \equiv \frac{2-s}{q_0 A_0 \gamma_2^{3-s}}, \tag{23}$$

and

$$\begin{aligned} t_{\rm K} &= \frac{s-1}{3-s} t_{\rm M}\left[\left(\frac{\gamma_2}{\gamma_1}\right)^{3-s} + \frac{2(2-s)}{s-1}\right] \\ &\simeq \frac{s-1}{3-s}\left(\frac{\gamma_2}{\gamma_1}\right)^{3-s} t_{\rm M} \gg t_{\rm M}, \end{aligned} \tag{24}$$

both of which are inversely proportional to the particle injection rate q_0. Using Eq. (18) we can express the time scale (23) in terms of the kinetic energy density of the injected particles as

$$t_{\rm M} = (A_0 K \gamma_2)^{-1}. \tag{25}$$

For flat spectral indices $s < 2$, the kinetic energy density K is determined by the upper cut-off γ_2 of the injected particles, which explains the appearance of γ_2 instead of γ_1 in the time scale (25). As an aside: if we compare the time scales (25) and (17) we notice that $t_{\rm M} = (\gamma_2/\gamma_1) t_{\rm L}$ is much shorter than $t_{\rm L}$.

Equation (13) then yields

$$\begin{aligned} T(0 \le t \le t_{\rm M}) &\simeq \frac{1}{\gamma_2}\frac{t}{t_{\rm M}}, \\ T(t_{\rm M} \le t \le t_{\rm K}) &\simeq \frac{1}{\gamma_2}\left[\frac{3-s}{s-1}\frac{t}{t_{\rm M}} - \frac{2(2-s)}{s-1}\right]^{1/(3-s)}, \\ T(t \ge t_{\rm K}) &\simeq \left[\gamma_2^{s-3}\gamma_1^{1-s}\left(\frac{2(2-s)}{s-1}\frac{t}{t_{\rm M}} - \frac{4(2-s)^2}{(3-s)(s-1)}\right) + \frac{s-1}{(3-s)\gamma_1^2}\right]^{1/2}. \end{aligned} \tag{26}$$

The approximate solution to the nonlinear kinetic equation is then

$$n(\gamma, 0 \le t \le t_{\rm M}, 1 < s < 2) \simeq q_0 \gamma^{-s}\left[1 - \frac{\gamma}{\gamma_2}\frac{t}{t_{\rm M}}\right]^{s-2} \times H\left[\frac{\gamma_2}{1+\frac{t}{t_{\rm M}}} - \gamma\right] H\left[\gamma - \frac{\gamma_1}{1+\frac{\gamma_1}{\gamma_2}\frac{t}{t_{\rm M}}}\right] H\left[\gamma_2\frac{t_{\rm M}}{t} - \gamma\right], \tag{27}$$

$$n(\gamma, t_{\rm M} \le t \le t_{\rm K}, 1 < s < 2) \simeq q_0 \gamma^{-s}\left[1 - \frac{\gamma}{\gamma_2}D(t)\right]^{s-2} \times H\left[\frac{\gamma_2}{1+D(t)} - \gamma\right] H\left[\gamma - \frac{\gamma_1}{1+\frac{\gamma_1}{\gamma_2}D(t)}\right] H\left[\frac{\gamma_2}{D(t)} - \gamma\right], \tag{28}$$

and

$$n(\gamma, t \ge t_{\rm K}, 1 < s < 2) \simeq q_0 \gamma^{-s}\left[1 - \frac{\gamma}{\gamma_2}F(t)\right]^{s-2} \times H\left[\frac{\gamma_2}{1+F(t)} - \gamma\right] H\left[\gamma - \frac{\gamma_1}{1+\frac{\gamma_1}{\gamma_2}F(t)}\right] H\left[\frac{\gamma_2}{F(t)} - \gamma\right] \tag{29}$$

where

$$D(t) = \left(\frac{3-s}{s-1}\frac{t}{t_{\rm M}} - \frac{2(2-s)}{s-1}\right)^{1/(3-s)}, \tag{30}$$

and

$$\begin{aligned} F(t) &= \left[\left(\frac{\gamma_2}{\gamma_1}\right)^{s-1}\left[\frac{2(2-s)}{s-1}\frac{t}{t_{\rm M}} - \frac{4(2-s)^2}{(3-s)(s-1)}\right] \right. \\ &\quad \left. + \frac{s-1}{(3-s)}\left(\frac{\gamma_2}{\gamma_1}\right)^2\right]^{1/2}. \end{aligned} \tag{31}$$

Again the solutions are continous at $t = t_{\rm M}$ and $t = t_{\rm K}$, respectively.

5. Properties of the nonlinear electron distribution function in comparison to the linear electron distribution

In this section we discuss in detail the differences between the properties of the nonlinear and the linear solutions regarding the cooling time scales, the time evolution of the upper and lower cut-offs in the electron distribution and the distribution function itself.

5.1. Cooling time scales

In the linear cooling case, solution (8) shows that an electron starting with Lorentz factor γ_2 cools to the Lorentz factor

$$\gamma_{\rm L} = \frac{\gamma_2}{1 + D_0\gamma_2 t} \tag{32}$$

at later times. The half-life time, $t^{\rm L}_{1/2}$, where the Lorentz factor has cooled to half its initial value $\gamma_{\rm L}(t^{\rm L}_{1/2}) = \gamma_2/2$,

$$t^{\rm L}_{1/2} = \frac{1}{D_0\gamma_2} = \frac{3.76\times10^{13}}{\gamma_2}\left[\frac{4.54\ {\rm mG}}{B}\right]^2 {\rm s}, \tag{33}$$

depends inversely on the initial Lorentz factor and the magnetic field strength. In particular, $t^{\rm L}_{1/2}$ does not dependent on the strength q_0 of the injection rate or the initial kinetic energy in injected electrons K.

In the nonlinear cooling case, the time dependence of the electron distribution function is controlled by the time scale (25)

$$t_{\rm M} = (A_0\gamma_2 K)^{-1} = \frac{3}{4c\sigma_{\rm T}e_B K\gamma_2}$$
$$= 3.76\times10^{13}e_B^{-1}\gamma_2^{-1}\left[K/{\rm cm}^{-3}\right]^{-1} \quad {\rm s}. \tag{34}$$

Here $t_{\rm M}$ does depend on the initial kinetic energy of injected electrons K due to the equipartition conditions. The more electrons that are injected, the quicker each electron cools under equipartition requirements. Such a collective behaviour is new and completely different from the linear case.

5.1.1. Non-equipartition conditions

For non-equipartition magnetic field strengths, the ratio of the nonlinear (34) to the linear (33) cooling time

$$r = \frac{t_{\rm M}}{t^{\rm L}_{1/2}} = \frac{1}{e_B K}\left[\frac{B}{4.54\ {\rm mG}}\right]^2 \tag{35}$$

is much lower than unity provided $Ke_B > \left[\frac{B}{4.54\ {\rm mG}}\right]^2$, which is easily fulfilled in GRB sources and blazars. Modelling of blazar flaring (e.g. Dermer & Schlickeiser 1992, 2002) indicates that about $q_0 \simeq 10^5$ electrons per cm^{-3} with Lorentz factors $\gamma_2 \simeq 10^7$, implying $K = 10^{12}$ cm^{-3}, are injected into sources with several Gauss ($B \simeq 10$ G) fields. The nonlinear cooling time is then more than four orders of magnitude shorter than the standard linear half-life (SL).

5.1.2. Equipartition conditions

In equipartition conditions with constant energy density ratio values,

$$e_B = e_B(0) = \frac{U_B(0)}{U_{\rm e}(0)} = \frac{B^2(0)}{8\pi m_{\rm e}c^2 K}, \tag{36}$$

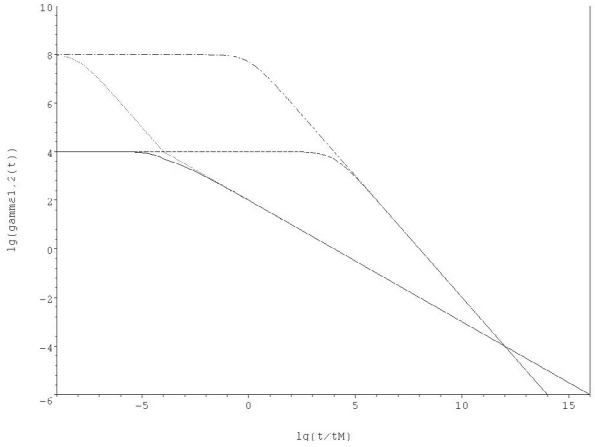

Fig. 3. Time dependences of the lower ($\gamma_1(t)$) and the upper ($\gamma_2(t)$) cut-offs of the electron distribution functions for $s = 3$ in the linear and nonlinear case. Linear $\gamma_1(t)$ (dashed curve), nonlinear $\gamma_1(t)$ (thick full curve), linear $\gamma_2(t)$ (dotted-dashed curve), nonlinear $\gamma_2(t)$ (thin full curve). Initial values $\gamma_1 = 10^4$ and $\gamma_2 = 10^8$ are assumed.

the initial magnetic field strength $B(0)$ is determined by the initial kinetic energy of injected particles, so that the cooling time ratio (35) equals unity,

$$r_{\rm eq} = 1, \tag{37}$$

implying equal nonlinear and linear cooling time values $t_{\rm M} = t^{\rm L}_{1/2}$.

To illustrate the results in the following, we adopt initial electron cut-offs $\gamma_1 = 10^4$ and $\gamma_2 = 10^8$ and the full equipartition parameters $K = 10^{12}$ cm^{-3}, implying $B(0) = 4.53\times10^3$ G. In this case the linear and nonlinear cooling time values are equal, $t_{\rm M} = t^{\rm L}_{1/2}$.

5.2. Electron distribution function cut-offs

In the linear cooling case, the Lorentz factor cut-offs γ_1 and γ_2 of the initial power law each decrease as a function of time as

$$\gamma^{\rm L}_1(t) = \frac{\gamma_1}{1+\gamma_1 D_0 t}, \quad \gamma^{\rm L}_2(t) = \frac{\gamma_2}{1+\gamma_2 D_0 t}\cdot \tag{38}$$

In terms of the nonlinear time scale $t_{\rm M}$, Eqs. (38) read as

$$\gamma^{\rm L}_1(t) = \frac{\gamma_1}{1+\frac{\gamma_1}{\gamma_2}\frac{t}{t_{\rm M}}}, \quad \gamma^{\rm L}_2(t) = \frac{\gamma_2}{1+\frac{t}{t_{\rm M}}}\cdot \tag{39}$$

In the nonlinear case we find for steep injection spectra $s > 2$

$$\gamma^{\rm NL}_1(t) = \begin{cases} \dfrac{\gamma_1}{1+\frac{\gamma_1}{\gamma_2}\frac{t}{t_{\rm M}}} & \text{for } 0 \le t \le \frac{\gamma_1}{\gamma_2}t_{\rm M} \\ \dfrac{\gamma_1}{1+\left[\frac{2(s-2)}{s-1}\frac{\gamma_2 t}{\gamma_1 t_{\rm M}}+\frac{3-s}{s-1}\right]^{1/2}} & \text{for } t \ge \frac{\gamma_1}{\gamma_2}t_{\rm M} \end{cases} \tag{40}$$

and

$$\gamma^{\rm NL}_2(t) = \begin{cases} \dfrac{\gamma_2}{1+(\frac{\gamma_2}{\gamma_1})^2\frac{t}{t_{\rm M}}} & \text{for } 0 \le t \le \frac{\gamma_1}{\gamma_2}t_{\rm M} \\ \dfrac{\gamma_2}{1+\frac{\gamma_2}{\gamma_1}\left[\frac{2(s-2)}{s-1}\frac{\gamma_2 t}{\gamma_1 t_{\rm M}}+\frac{3-s}{s-1}\right]^{1/2}} & \text{for } t \ge \frac{\gamma_1}{\gamma_2}t_{\rm M}. \end{cases} \tag{41}$$

Figure 3 displays the different time dependences of $\gamma_1(t)$ and $\gamma_2(t)$ for the linear and the nonlinear cases, calculated for $s = 3$. We note several important differences: (a) at early times $t \le \frac{\gamma_1}{\gamma_2}t_{\rm M} = 10^{-4}t_{\rm M}$, the nonlinear lower cut-off value is practically

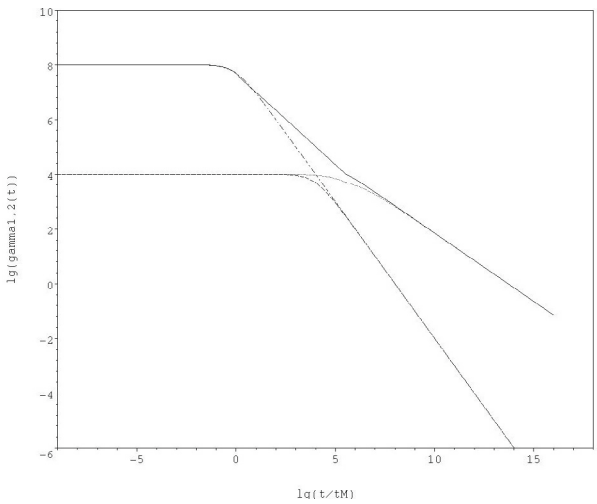

Fig. 4. Time dependences of the lower ($\gamma_1(t)$) and the upper ($\gamma_2(t)$) cut-offs of the electron distribution functions for $s = 1.5$ in the linear and nonlinear cases. Linear $\gamma_1(t)$ (dashed curve), nonlinear $\gamma_1(t)$ (thin full curve), linear $\gamma_2(t)$ (dotted-dashed curve), nonlinear $\gamma_2(t)$ (thick full curve). Initial values $\gamma_1 = 10^4$ and $\gamma_2 = 10^8$ are assumed.

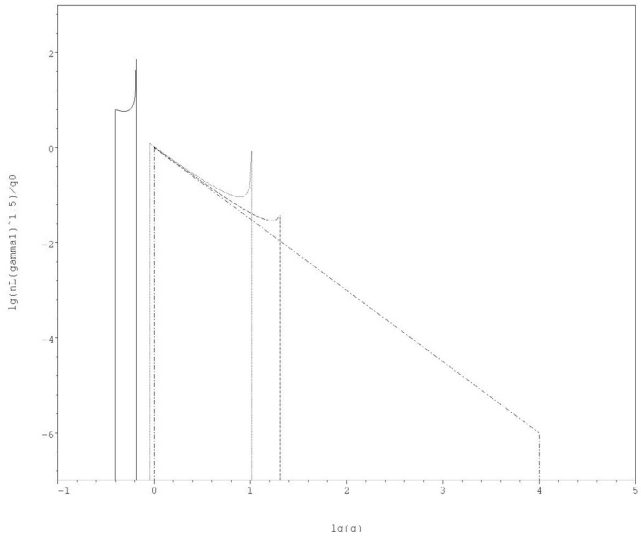

Fig. 5. Electron distribution function $n_{\rm NL}\gamma_1^{3/2}/q_0$ as a function of the normalised Lorentz factor $g = \gamma/\gamma_1$ for $s = 1.5$ and $g_2 = \gamma_2/\gamma_1 = 10^4$ in the nonlinear cooling case at different times $\tau = t/t_{\rm M} = 0$ (dotted-dashed curve), 10^2 (dashed curve), 10^4 (thin full curve), and 10^6 (thick full curve).

constant as is the linear lower cut-off value; (b) at early times $t \le \frac{\gamma_1}{\gamma_2} t_{\rm M} = 10^{-4} t_{\rm M}$, the linear upper cut-off value remains practically constant while the nonlinear upper cut-off quickly decreases inversely proportional to time; (c) at later times, the upper and lower cut-off curves converge to each other both in the linear and nonlinear cases; i.e., the initially broad power law is significantly quenched, but the nonlinear cut-offs exhibit a slower ($\propto t^{-1/2}$) decay than the linear decrease in the linear cut-offs.

Likewise, in the nonlinear case, we find for flat injection spectra $1 < s < 2$

$$\gamma_1^{\rm NL}(t) = \begin{cases} \frac{\gamma_1}{1+\frac{\gamma_1}{\gamma_2}\frac{t}{t_{\rm M}}} & \text{for } 0 \le t \le t_{\rm M} \\ \frac{\gamma_1}{1+\frac{\gamma_1}{\gamma_2}D(t)} & \text{for } t_{\rm M} \le t \le \frac{s-1}{3-s}\left(\frac{\gamma_2}{\gamma_1}\right)^{3-s} t_{\rm M} \\ \frac{\gamma_1}{1+\frac{\gamma_1}{\gamma_2}F(t)} & \text{for } t \ge \frac{s-1}{3-s}(\frac{\gamma_2}{\gamma_1})^{3-s} t_{\rm M} \end{cases} \tag{42}$$

and

$$\gamma_2^{\rm NL}(t) = \begin{cases} \frac{\gamma_2}{1+\frac{t}{t_{\rm M}}} & \text{for } 0 \le t \le t_{\rm M} \\ \frac{\gamma_2}{1+D(t)} & \text{for } t_{\rm M} \le t \le \frac{s-1}{3-s}(\frac{\gamma_2}{\gamma_1})^{3-s} t_{\rm M} \\ \frac{\gamma_2}{1+F(t)} & \text{for } t \ge \frac{s-1}{3-s}(\frac{\gamma_2}{\gamma_1})^{3-s} t_{\rm M} \end{cases} , \tag{43}$$

which are shown in Fig. 4 for $s = 1.5$ in comparison to the linear behaviour. Again at early times, $t \le t_{\rm M}$, the cut-off variations with time are similar to the linear case, while at intermediate times, they exhibit a power law decrease through $D(t)$ (depending on the spectral index s of injected particles). At late times, $t \ge \frac{s-1}{3-s}(\frac{\gamma_2}{\gamma_1})^{3-s} t_{\rm M}$, they exhibit a decrease through $F(t)$.

5.3. Electron distribution function

For the same parameters used in the last section, we show in Figs. 5 and 6 the nonlinear and linear electron distributions as a function of the electron Lorentz factor for the cases $s = 1.5$ and $s = 3$. Again the power laws appear between sharp lower and upper cut-offs that decrease with time. One also notices the significant quenching of the power law with increasing time and the pile-up in the case of flat injection spectral index (Fig. 5).

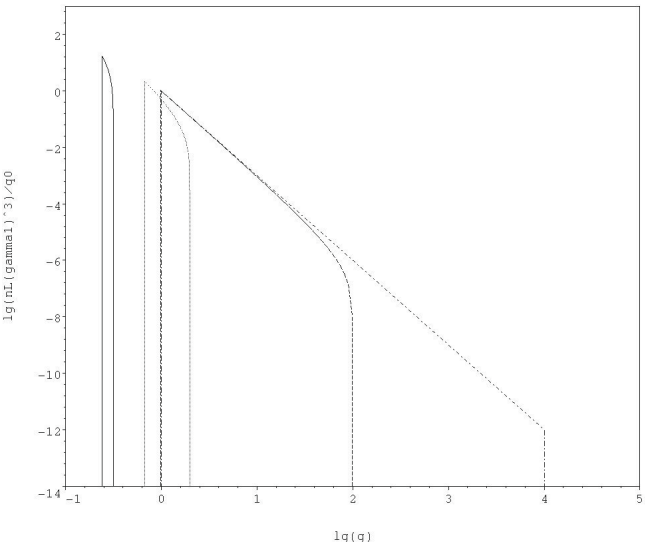

Fig. 6. Electron distribution function $n_{\rm NL}\gamma_1^3/q_0$ as a function of the normalised Lorentz factor $g = \gamma/\gamma_1$ for $s = 3$ and $g_2 = \gamma_2/\gamma_1 = 10^4$ in the nonlinear cooling case at different times $\tau = t/t_{\rm M} = 0$ (dotted-dashed curve), 10^{-2} (dashed curve), 0.5 (thin full curve), and 10 (thick full curve).

6. Electron fluence distribution

In this section we calculate the time-integrated electron distributions (fluences)

$$N(\gamma) = \int_0^\infty {\rm d}t\, n(\gamma, t) \tag{44}$$

in the linear and nonlinear cases.

6.1. Linear electron fluence

With the substitution $\tau = D_0\gamma t$, the linear distribution function (8) immediately yields

$$N_{\rm L}(\gamma) = \frac{q_0}{D_0}\gamma^{-(s+1)}\int_0^\infty {\rm d}\tau(1-\tau)^{s-2}H\left[\tau - \frac{\gamma_1-\gamma}{\gamma_1}\right]$$

$$\times\, H\left[\frac{\gamma_2-\gamma}{\gamma_2} - \tau\right] = \frac{q_0}{D_0(s-1)}$$

$$\times\begin{cases}\gamma^{-2}\left[\gamma_1^{1-s}-\gamma_2^{1-s}\right] & \text{for } 0\le\gamma\le\gamma_1\\ \gamma^{-(s+1)}\left[1-(\frac{\gamma}{\gamma_2})^{s-1}\right] & \text{for } \gamma_1\le\gamma\le\gamma_2\\ 0 & \text{for } \gamma>\gamma_2.\end{cases} \quad (45)$$

This broken power law exhibits a spectral break by $\Delta s = s-1$ at γ_1.

6.2. Nonlinear electron fluence

The nonlinear distribution functions (20)–(21) for large spectral indices $s > 2$, and (27)–(29) for flat spectral spectral indices $1 < s < 2$, are used in Appendix C to calculate the nonlinear electron fluence distributions.

For electron radiation processes not subject to equipartition conditions, such as inverse Compton scattering of ambient photon gases and relativistic bremsstrahlung, the energy dependences of the electron number density and the electron fluence can be directly used to infer the frequency dependence of the fluxes and fluences of the generated photons by folding the electron energy distributions with the respective radiation cross-sections to calculate the respective spontaneous emission and absorption coefficients.

In the case of synchrotron radiation and synchrotron-self-Compton emission, the frequency-energy relation is more complicated as the magnetic field strength is also time-dependent due to the equipartition condition. In Sect. 8 we calculate the nonlinear optically thin synchrotron radiation intensity and compare it with the synchrotron intensity in the linear cooling case.

With the substitutions $z = t/t_{\rm L}$, $g = \gamma/\gamma_1$ and $g_2 = \gamma_2/\gamma_1$ for large spectral indices, we obtain

$$N_{\rm NL}(\gamma>\gamma_2, s>2) = 0,$$
$$N_{\rm NL}(\gamma_1<\gamma\le\gamma_2, s>2) = \frac{q_0 t_{\rm L}\gamma_1}{s-1}\gamma^{-s-1}\left[1-\left(\frac{\gamma}{\gamma_2}\right)^{s-1}\right] \quad (46)$$

$$N_{\rm NL}\left(\frac{\gamma_2}{1+\gamma_2}<\gamma\le\gamma_1, s>2\right) = \frac{q_0 t_{\rm L}\gamma_1^{2-s}}{s-1}\gamma^{-2}\left[1-\left(\frac{\gamma_1}{\gamma_2}\right)^{s-1}\right] \quad (47)$$

$$N_{\rm NL}\left(\frac{\gamma_1}{2}<\gamma\le\frac{\gamma_2}{1+\gamma_2}, s>2\right) = q_0 t_{\rm L}\gamma^{-s}$$

$$\times\left[\frac{1}{g(s-1)}\left[g^{s-1}-(1-g)^{s-1}\right]+\frac{s-1}{g^2(s-2)}\right.$$

$$\left.\times\left[\frac{(1-g)^{s-1}-g^{s-1}g_2^{1-s}}{s-1}-\frac{(1-g)^s-g^s g_2^{-s}}{s}\right]\right] \quad (48)$$

and

$$N_{\rm NL}\left(\gamma\le\frac{\gamma_1}{2}, s>2\right) = \frac{q_0 t_{\rm L}\gamma_1^{3-s}}{s-2}\gamma^{-3}\left(1-\left(\frac{\gamma_1}{\gamma_2}\right)^{s-1}\right.$$

$$\left.-\frac{s-1}{s}\frac{\gamma}{\gamma_1}\left[1-\left(\frac{\gamma_1}{\gamma_2}\right)^s\right]\right)$$

$$\simeq \frac{q_0 t_{\rm L}\gamma_1^{3-s}}{s-2}\gamma^{-3}\left(1-\frac{s-1}{s}\frac{\gamma}{\gamma_1}\right). \quad (49)$$

For the Lorentz factors above γ_1, the nonlinear fluence distribution agrees with the linear steepened injection distribution (49), but for lower energies we obtain a different behaviour. Much below the transition region $\gamma \simeq \gamma_1/2$, the nonlinear fluence (154) approaches a power law $\propto\gamma^{-3}$ whose spectral index is larger by unity than in the linear case. Consequently, we also obtain a broken power-law behaviour for the nonlinear fluence, but with a smaller spectral break by $\Delta s = s-2$ around γ_1 than in the linear case.

Likewise, for flat injection spectra we find

$$N_{\rm NL}(g, 1<s<2) = q_0 t_{\rm M}\gamma_1^{-s}J(g) \quad (50)$$

with

$$J(g>g_2) = 0,$$
$$J\left(\frac{g_2}{2}\le g\le g_2\right) = \frac{g_2}{s-1}g^{-(s+1)}\left[1-(g/g_2)^{s-1}\right], \quad (51)$$

$$J\left(1\le g\le\frac{g_2}{2}\right) = g_2 g^{-(s+1)}\left[\frac{1-(1-\frac{g}{g_2})^{s-1}}{s-1}\right]$$

$$+\,(g_2/g)^{2-s}\left[\left(1-\frac{g}{g_2}\right)^{s-1}-\left(\frac{g}{g_2}\right)^{s-1}\right]$$

$$\simeq g_2^{3-s}g^{-3}\left[\left(1-\frac{g}{g_2}\right)^{s-1}-\left(\frac{g}{g_2}\right)^{s-1}\right] \quad (52)$$

and

$$J\left(g\le\frac{1}{2}\right)\simeq\frac{g_2^{3-s}}{2-s}g^{-3}\left[1-\frac{s-1}{s}g\right], \quad (53)$$

which, at all energies less than $g \le (g_2/2)$ corresponding to $\gamma\le\gamma_2/2$, is an unbroken power law with spectral index 3 independent of the injected flat power law value $1 < s < 2$.

7. Steady-state case

For completeness here we consider the linear and nonlinear steady-state solutions for the electron distribution resulting from the steady injection of the power law

$$Q(\gamma) = q_0\gamma^{-s}H[\gamma-\gamma_1]H[\gamma_2-\gamma] \quad (54)$$

with $\gamma_2 > \gamma_1 \gg 1$. The linear electron equilibrium distribution obeys the kinetic equation

$$\frac{\rm d}{{\rm d}\gamma}\left[D_0\gamma(\gamma^2-1)^{1/2}M_{\rm L}(\gamma)\right] = -Q(\gamma), \quad (55)$$

whereas the nonlinear electron equilibrium distribution obeys

$$A_0\left[\int_1^\infty \mathrm{d}u\left[(u^2-1)^{1/2}-1\right]M_\mathrm{N}(u)\right]$$
$$\times\frac{\mathrm{d}}{\mathrm{d}\gamma}(\gamma\left(\gamma^2-1\right)^{1/2}M_\mathrm{N}(\gamma)\Big)=-Q(\gamma). \quad (56)$$

In contrast to the previous calculations, we depart from the ultrarelativistic treatment, so that $1\le\gamma\le\infty$, and we use the correspondingly corrected forms for the kinetic energy density and the synchrotron loss term (Kirk et al. 1988). The linear kinetic Eq. (55) immediately yields

$$\begin{aligned}M_\mathrm{L}(\gamma) &= \frac{1}{D_0\gamma\left(\gamma^2-1\right)^{1/2}}\int_\gamma^\infty \mathrm{d}\gamma' Q\left(\gamma'\right)\\ &= \frac{q_0}{D_0(s-1)\gamma\left(\gamma^2-1\right)^{1/2}}\\ &\times\begin{cases}\gamma_1^{1-s}[1-(\gamma_1/\gamma_2)^{s-1}] & \text{for } \gamma\le\gamma_1\\ \gamma^{1-s}[1-(\gamma/\gamma_2)^{s-1}] & \text{for } \gamma_1\le\gamma\le\gamma_2\\ 0 & \text{for } \gamma\ge\gamma_2.\end{cases}\end{aligned} \quad (57)$$

To solve the nonlinear kinetic Eq. (56) introduce

$$S(\gamma)=\gamma(\gamma^2-1)^{1/2}M_\mathrm{N}(\gamma) \quad (58)$$

and

$$\begin{aligned}U &= \int_1^\infty \mathrm{d}\gamma\left[\left(\gamma^2-1\right)^{1/2}-1\right]M_\mathrm{N}(\gamma)\\ &= \int_1^\infty \mathrm{d}\gamma\left[\left(\gamma^2-1\right)^{1/2}-1\right]\gamma^{-1}(\gamma^2-1)^{-1/2}S(\gamma),\end{aligned} \quad (59)$$

so that Eq. (56) reads

$$\frac{\mathrm{d}S}{\mathrm{d}\gamma}=-\frac{Q(\gamma)}{A_0U} \quad (60)$$

with the solution

$$\begin{aligned}S(\gamma) &= \frac{1}{A_0U}\int_\gamma^\infty \mathrm{d}\gamma' Q(\gamma')\\ &= \frac{q_0}{(s-1)A_0U}\begin{cases}\gamma_1^{1-s}-\gamma_2^{1-s} & \text{for } \gamma\le\gamma_1\\ \gamma^{1-s}-\gamma_2^{1-s} & \text{for } \gamma_1\le\gamma\le\gamma_1\\ 0 & \text{for } \gamma\ge\gamma_2.\end{cases}\end{aligned} \quad (61)$$

Inserting Eq. (61) yields for Eq. (59)

$$U^2=\frac{q_0}{A_0(s-1)}\Big(\left[\gamma_1^{1-s}-\gamma_2^{1-s}\right]\int_1^{\gamma_1}\frac{\mathrm{d}\gamma}{\gamma}$$
$$-\int_{\gamma_1}^{\gamma_2}\mathrm{d}\gamma\frac{\gamma^{-s}}{\left(\gamma^2-1\right)^{1/2}}+\gamma_2^{1-s}\int_{\gamma_1}^{\gamma_2}\mathrm{d}\gamma\gamma^{-1}(\gamma^2-1)^{-1/2}\Big). \quad (62)$$

Because $\gamma_1\gg1$ the second and third integral in Eq. (62) are solved approximately as

$$\int_{\gamma_1}^{\gamma_2}\mathrm{d}\gamma\gamma^{-s}\left(\gamma^2-1\right)^{-1/2}\simeq\int_{\gamma_1}^{\gamma_2}\mathrm{d}\gamma\gamma^{-s-1}\simeq\frac{1}{s}\left(\gamma_1^{-s}-\gamma_2^{-s}\right)$$

and

$$\int_{\gamma_1}^{\gamma_2}\mathrm{d}\gamma\gamma^{-1}\left(\gamma^2-1\right)^{-1/2}\simeq\int_{\gamma_1}^{\gamma_2}\mathrm{d}\gamma\gamma^{-2}=\gamma_1^{-1}-\gamma_2^{-1}.$$

We then obtain

$$\begin{aligned}U^2 &\simeq \frac{q_0}{A_0(s-1)}\Big(\left[\gamma_1^{1-s}-\gamma_2^{1-s}\right]\ln\gamma_1\\ &-\frac{1}{s}\left(\gamma_1^{-s}-\gamma_2^{-s}\right)+\gamma_2^{1-s}\left(\gamma_1^{-1}-\gamma_2^{-1}\right)\Big).\end{aligned} \quad (63)$$

The nonlinear solution according to Eqs. (58) and (61) then is

$$\begin{aligned}M_\mathrm{N}(\gamma) &= \frac{q_0}{(s-1)A_0U}\gamma^{-1}\left(\gamma^2-1\right)^{-1/2}\\ &\times\begin{cases}\gamma_1^{1-s}-\gamma_2^{1-s} & \text{for } \gamma\le\gamma_1\\ \gamma^{1-s}-\gamma_2^{1-s} & \text{for } \gamma_1\le\gamma\le\gamma_1\\ 0 & \text{for } \gamma\ge\gamma_2.\end{cases}\end{aligned} \quad (64)$$

For $\gamma_2\gg\gamma_1\gg1$ and $s>1$ we find approximately

$$U\simeq\left[\frac{q_0\ln\gamma_1}{A_0(s-1)\gamma_1^{s-1}}\right]^{1/2} \quad (65)$$

and

$$\begin{aligned}M_\mathrm{N}(\gamma) &\simeq \frac{q_0^{1/2}\gamma_1^{(s-1)/2}}{[A_0(s-1)\ln\gamma_1]^{1/2}}\gamma^{-1}\left(\gamma^2-1\right)^{-1/2}\\ &\times\begin{cases}\gamma_1^{1-s}-\gamma_2^{1-s} & \text{for } \gamma\le\gamma_1\\ \gamma^{1-s}-\gamma_2^{1-s} & \text{for } \gamma_1\le\gamma\le\gamma_1\\ 0 & \text{for } \gamma\ge\gamma_2.\end{cases}\end{aligned} \quad (66)$$

Under equipartition conditions (see Sect. 5.1.2), we have

$$D_0=A_0K=\frac{q_0}{2-s}\left(\gamma_2^{2-s}-\gamma_1^{2-s}\right)A_0, \quad (67)$$

yielding for the linear solution (56)

$$\begin{aligned}M_\mathrm{L}(\gamma) &= \frac{2-s}{A_0(s-1)\left(\gamma_2^{2-s}-\gamma_1^{2-s}\right)}\gamma^{-1}\left(\gamma^2-1\right)^{-1/2}\\ &\times\begin{cases}\gamma_1^{1-s}-\gamma_2^{1-s} & \text{for } \gamma\le\gamma_1\\ \gamma^{1-s}-\gamma_2^{1-s} & \text{for } \gamma_1\le\gamma\le\gamma_2\\ 0 & \text{for } \gamma\ge\gamma_2.\end{cases}\end{aligned} \quad (68)$$

While the linear (Eq. (68)) and the nonlinear (Eq. (66)) steady-state solutions exhibit the same dependence on the electron Lorentz factor, their absolute values are different. The nonlinear solution (66) depends on the injection rate ($\propto q_0^{1/2}$) whereas the linear solution (68) under equipartition conditions is independent from q_0. Also the dependence on the initial cut-offs γ_1 and γ_2 is different for the two solutions.

8. Optically thin synchrotron intensity and fluence distribution

Here we calculate the optically thin synchrotron intensity and fluence distribution in the linear and nonlinear cooling case, using the monochromatic approximation (Felten & Morrison 1966) of the synchrotron spectral power in vacuum

$$p_\mathrm{syn}(\gamma,\nu)=\frac{c\sigma_\mathrm{T}B^2\gamma^2}{6\pi}\delta(\nu-\nu_s\gamma^2) \quad (69)$$

with the characteristic frequency

$$\nu_s=\frac{3eB}{4\pi m_\mathrm{e}c}=4.2\times10^6 b\quad\mathrm{Hz} \quad (70)$$

for a magnetic field strength of $B = b$ Gauss. Here, σ_T denotes the Thomson cross section. The monochromatic approxiamtion works well for broad energy distribution functions of the radiating electrons, as is the case here.

The optically thin synchrotron radiation intensity from a homogeneous source of size L is then given as

$$I(\nu,t) = \frac{L}{4\pi}\int_0^\infty \mathrm{d}\gamma n(\gamma,t) p_{\rm syn}(\gamma,\nu) = \frac{Lc\sigma_T B^2}{48\pi^2\nu_s}\sqrt{\frac{\nu}{\nu_s}}\, n\left(\gamma=\sqrt{\frac{\nu}{\nu_s}},t\right). \quad (71)$$

8.1. Linear cooling

With the linear electron distribution function (8), we obtain

$$I_L(\nu,t) = \frac{Lcq_0\sigma_T B^2}{48\pi^2\nu_s}\left(\frac{\nu}{\nu_s}\right)^{\frac{1-s}{2}}\left[1-D_0 t\sqrt{\frac{\nu}{\nu_s}}\right]^{s-2} H[t] \times H\left[\nu-\frac{\nu_s\gamma_1^2}{(1+D_0\gamma_1 t)^2}\right] H\left[\frac{\nu_s\gamma_2^2}{(1+D_0\gamma_2 t)^2}-\nu\right]. \quad (72)$$

Using our previous notation $g_2 = \gamma_2/\gamma_1$ and $\tau = D_0\gamma_1 t$ and introducing the normalised frequency

$$\omega = \frac{\nu}{\nu_s\gamma_1^2}, \quad (73)$$

we can write the linear synchrotron intensity (72) as

$$I_L(\omega,\tau) = \frac{Lcq_0\sigma_T B^2}{48\pi^2\nu_s\gamma_1^{s-1}}\omega^{\frac{1-s}{2}}\left[1-\tau\omega^{1/2}\right]^{s-2} H[\tau] \times H\left[\omega-(1+\tau)^{-2}\right] H\left[\left(\frac{g_2}{1+g_2\tau}\right)^2-\omega\right]. \quad (74)$$

By integrating over all times we obtain for the linear synchrotron fluence

$$F_L(\omega) = \frac{1}{D_0\gamma_1}\int_0^\infty \mathrm{d}\tau I_L(\omega,\tau) = \frac{Lcq_0\sigma_T B^2}{48(s-1)\pi^2 D_0\nu_s\gamma_1^s} \times \begin{cases} \omega^{-1/2}(1-g_2^{1-s}) & \text{for } \omega \le 1 \\ \omega^{-s/2}[1-(\omega/g_2^2)^{(s-1)/2}] & \text{for } 1 \le \omega \le g_2^2. \end{cases} \quad (75)$$

The linear synchrotron fluence is a broken power law THAT exhibits a spectral break by $\Delta\alpha = (s-1)/2$ at $\nu = \nu_s\gamma_1^2$ in agreement with the behaviour of the linear electron fluence (45). Moreover, independent of the spectral index s of the injected power law, the linear synchrotron fluence at low frequencies approaches the same frequency spectral index $\alpha_L = 0.5$.

8.2. Nonlinear cooling

In the nonlinear cooling case the magnetic field strength becomes time-dependent (see Eq. (2)) so that the characteristic frequency (70) is

$$\nu_s(t) = K_0[U(t)]^{1/2} \ \text{Hz} \quad (76)$$

with ($y = A_0 t$)

$$U(y) = \int_0^\infty \mathrm{d}\gamma\gamma n(\gamma,t) = \frac{\mathrm{d}T}{\mathrm{d}y}, \quad (77)$$

and in terms of the classical electron radius r_0

$$K_0 = 3c\sqrt{\frac{e_B r_0}{2\pi}} = 1.9\times10^4 \ \ \text{Hz cm}^{3/2}. \quad (78)$$

The optically thin synchrotron radiation intensity from a homogeneous source of size L is then given as

$$I_{NL}(\nu,y) = \frac{Lm_e c^3\sigma_T e_B U^{1/2}(y)}{6\pi K_0}\sqrt{\frac{\nu}{K_0U^{1/2}(y)}} \times n\left(\gamma=\sqrt{\frac{\nu}{K_0U^{1/2}(y)}},y\right). \quad (79)$$

Inserting the nonlinear electron distribution function (11) we find

$$I_{NL}(\nu,y) = \frac{Lm_e c^3\sigma_T q_0 e_B U^{1/2}(y)}{6\pi K_0}\left(\frac{\nu}{K_0U^{1/2}(y)}\right)^{\frac{1-s}{2}} \times\left(1-\sqrt{\frac{\nu}{K_0U^{1/2}(y)}}T(y)\right)^{s-2} \times H[y]H\left[\nu-\frac{K_0U^{1/2}\gamma_1^2}{(1+\gamma_1 T)^2}\right] H\left[\frac{K_0U^{1/2}\gamma_2^2}{(1+\gamma_2 T)^2}-\nu\right]. \quad (80)$$

Equations (13) and (16) now give the implicit time variable $T(y)$ as a function of y from which we calculate

$$U(y) = \frac{\mathrm{d}T}{\mathrm{d}y} \quad (81)$$

yielding

$$U(0\le y\le y_2, s<2) \simeq \frac{q_0}{2-s}x_2^{s-2},$$

$$U(y_2\le y\le y_1, s<2) \simeq \frac{q_0}{(2-s)(s-1)} \times\left[\frac{3-s}{(2-s)(s-1)}q_0 y-\frac{2(2-s)}{s-1}x_2^{3-s}\right]^{(s-2)/(3-s)},$$

$$U(y\ge y_1, s<2) \simeq \frac{q_0 x_1^{s-1}}{s-1}\left[\frac{2q_0}{s-1}x_1^{s-1}y+\frac{s-1}{3-s}x_1^2 - \frac{4(2-s)^2}{(3-s)(s-1)}x_2^{3-s}x_1^{s-1}\right]^{-1/2}, \quad (82)$$

and for steep spectral index values $s > 2$

$$U(0\le y\le \frac{s-2}{q_0}x_1^{3-s}, s>2) \simeq \frac{q_0}{s-2}x_1^{s-2},$$

$$U(y\ge \frac{s-2}{q_0}x_1^{3-s}, s>2) \simeq \frac{q_0 x_1^{s-1}}{s-1}\left[\frac{2q_0}{s-1}x_1^{s-1}y+\frac{3-s}{s-1}x_1^2\right]^{-1/2}. \quad (83)$$

Inserting these dependences $T(y)$ and $U(y)$ in Eq. (80) yields the nonlinear synchrotron radiation intensity at any time y.

In the following we limit our discussion to the case of steep spectral indices $s > 2$ and leave the case of flat spectral indices to the interested reader.

At times $y \le y_3 = (s-2)\gamma_1^{s-3}/q_0$, we find $T = U_0 y$ with the constant

$$U_0 = \frac{q_0}{(s-2)\gamma_1^{s-2}} \tag{84}$$

so that

$$I_{\rm NL}(\nu, y \le y_3) = N_0 q_0 U_0^{(s+1)/4} \left(\frac{\nu}{K_0}\right)^{\frac{1-s}{2}} \left(1 - \sqrt{\frac{\nu}{K_0 U_0^{1/2}}} T\right)^{s-2}$$

$$\times H[y] H\left[\nu - \frac{K_0 U_0^{1/2}\gamma_1^2}{(1+\gamma_1 T)^2}\right] H\left[\frac{K_0 U_0^{1/2}\gamma_2^2}{(1+\gamma_2 T)^2} - \nu\right] \tag{85}$$

with the abbreviation

$$N_0 = \frac{L m_{\rm e} c^3 \sigma_{\rm T} e_B}{6\pi K_0} \,. \tag{86}$$

At late times $y \ge y_3$, we find

$$U(y) = \frac{q_0}{(s-1)\gamma_1^{s-1} T(y)} = \frac{(s-2)U_0}{(s-1)\gamma_1 T(y)},$$

$$T(y) = \left[\frac{2q_0}{s-1} x_1^{s-1} y + \frac{3-s}{s-1} x_1^2\right]^{1/2} \tag{87}$$

so that

$$I_{\rm NL}(\nu, y \ge y_3) = N_0 q_0 U_0^{(s+1)/4} \left(\frac{s-1}{s-2}\right)^{(s+1)/4} \left(\frac{\nu}{K_0}\right)^{\frac{1-s}{2}}$$

$$\times\ (\gamma_1 T)^{-(s+1)/4} \left(1 - \left(\frac{(s-1)\nu^2}{(s-2)K_0^2 U_0 \gamma_1^4}\right)^{1/4} (\gamma_1 T)^{5/4}\right)^{s-2}$$

$$\times\ H\left[\nu - \frac{K_0 U_0^{1/2}\gamma_1^2}{(1+\gamma_1 T)^2}\sqrt{\frac{s-2}{(s-1)\gamma_1 T}}\right]$$

$$\times\ H\left[\frac{K_0 U_0^{1/2}\gamma_2^2}{(1+\gamma_2 T)^2}\sqrt{\frac{s-2}{(s-1)\gamma_1 T}} - \nu\right]. \tag{88}$$

Here it is convenient to substitute $x = \gamma_1 T$ and to introduce the normalised frequency

$$f \equiv \frac{\nu}{K_0 U_0^{1/2}\gamma_1^2} \,. \tag{89}$$

Equations (85) and (88) then read

$$I_{\rm NL}(f, x \le 1) = \frac{N_0 q_0 U_0^{1/2}}{\gamma_1^{s-1}} f^{\frac{1-s}{2}} \left(1 - f^{1/2} x\right)^{s-2} H[x]$$

$$\times\ H\left[f - (x+1)^{-2}\right] H\left[(x + g_2^{-1})^{-2} - f\right] \tag{90}$$

and

$$I_{\rm NL}(f, x\ >\ 1) = \frac{N_0 q_0 U_0^{1/2}}{\gamma_1^{s-1}} \left[\frac{s-2}{s-1}\right]^{\frac{s+1}{4}}$$

$$\times\ f^{\frac{1-s}{2}} x^{-\frac{s+1}{4}} \left(1 - \left(\frac{s-1}{s-2}\right)^{1/4} f^{1/2} x^{5/4}\right)^{s-2}$$

$$\times\ H\left[f - \frac{(\frac{s-2}{s-1})^{1/2}}{x^{1/2}(x+1)^2}\right] H\left[\frac{(\frac{s-2}{s-1})^{1/2}}{x^{1/2}(x+g_2^{-1})^2} - f\right]. \tag{91}$$

The intensity distribution (90) at early times provides non-zero contributions for normalised frequencies $f \ge 1/4$. Apart from different overall, frequency, and time normalisations, its functional behaviour is identical to the linear cooling intensity distribution (74).

Nonlinear cooling behaviour only occurs at late time $x > 1$ through the second intensity distribution (91), which is non-zero only for frequencies $f < f_0$ where

$$f_0 = \left(\frac{s-1}{s-2}\right)^{1/2} \left(1 + g_2^{-1}\right)^{-2}, \tag{92}$$

which is lose to but smaller than unity. Hence, for frequencies $f \ge 1$ we will obtain a functional behaviour identical to the linear cooling case described by the first intensity distribution (90). For low frequencies $f < 1/4$, only the second intensity distribution (91) contributes, which is markedly different from the linear behaviour.

For the nonlinear synchrotron fluence, we infer

$$F_{\rm NL}(f) = \frac{1}{A_0}\int_0^\infty {\rm d}y\ I_{\rm NL}(f,y) = \frac{1}{A_0}\int_0^\infty {\rm d}T\ U^{-1}(T) I_{\rm NL}(f,T)$$

$$= \frac{N_0 q_0 f^{\frac{1-s}{2}}}{A_0 \gamma_1^s U_0^{1/2}} \left(\int_0^1 {\rm d}x \left(1 - f^{1/2}x\right)^{s-2}\right.$$

$$\times H\left[f - (x+1)^{-2}\right] H\left[(x+g_2^{-1})^{-2} - f\right]$$

$$+ \left[\frac{s-2}{s-1}\right]^{\frac{s-3}{4}} \int_1^\infty {\rm d}x\, x^{\frac{3-s}{4}} \left(1 - (\tfrac{s-1}{s-2})^{1/4} f^{1/2} x^{5/4}\right)^{s-2}$$

$$\left.\times\ H\left[f - \frac{(\frac{s-2}{s-1})^{1/2}}{x^{1/2}(x+1)^2}\right] H\left[\frac{(\frac{s-2}{s-1})^{1/2}}{x^{1/2}(x+g_2^{-1})^2} - f\right]\right), \tag{93}$$

which we evaluate in the two frequency regimes $f > 1$ and $f \ll 1/4$.

For frequencies $f > 1$, only the first term in Eq. (93) contributes yielding

$$F_{\rm NL}(f > 1) = \frac{N_0 q_0}{A_0 (s-1)\gamma_1^{s-1} U_0^{1/2}} f^{-\frac{s}{2}} \left[1 - (f/g_2^2)^{\frac{s-1}{2}}\right], \tag{94}$$

which apart from the overall normalisation ($\propto q_0^{1/2}$) and the different frequency normalisation, exhibits the linear cooling frequency dependence (compare with Eq. (75b)).

For frequencies $f \ll 1/4$ only the second term in Eq. (93) contributes. The two Heaviside functions in the second term limit the range of x to $X_1 \le x \le X_2$ with

$$X_1^{1/2}(X_1+1)^2 = \frac{(\frac{s-2}{s-1})^{1/2}}{f},$$

$$X_2^{1/2}(X_2+g_2^{-1})^2 = \frac{(\frac{s-2}{s-1})^{1/2}}{f} \,. \tag{95}$$

For $f \ll 1/4$ we find $X_2 > X_1 \gg 1$ so that

$$X_1 \simeq \frac{(\frac{s-2}{s-1})^{1/5}}{f^{2/5}} - 1, \quad X_2 \simeq \frac{(\frac{s-2}{s-1})^{1/5}}{f^{2/5}} - g_2^{-1}. \tag{96}$$

The nonlinear synchrotron fluence then is

$$F_{\rm NL}(f \ll 0.25) = \frac{N_0 q_0}{A_0 \gamma_1^s U_0^{1/2}} \left[\frac{s-2}{s-1}\right]^{\frac{s-3}{4}} f^{\frac{1-s}{2}} \int_{X_1}^{X_2} {\rm d}x\, g(x) \tag{97}$$

where

$$g(x) = x^{\frac{3-s}{4}} \left(1 - \left(\frac{s-1}{s-2}\right)^{1/4} f^{1/2} x^{5/4}\right)^{s-2}, \quad (98)$$

which we evaluate approximately as

$$\int_{X_1}^{X_2} \mathrm{d}x\, g(x) \simeq (X_2 - X_1) g(X_1)$$
$$\simeq \left(\frac{5}{4}\right)^{s-2} (1 - g_2^{-1}) \left(\frac{s-2}{s-1}\right)^{\frac{11-5s}{20}} f^{\frac{5s-11}{10}}. \quad (99)$$

For the fluence (97) at low frequencies, we find

$$F_{\rm NL}(f \ll 0.25) \simeq \left(\frac{5}{4}\right)^{s-2} \frac{N_0 q_0}{A_0 \gamma_1^s U_0^{1/2}} \left[\frac{s-2}{s-1}\right]^{-1/5} f^{-3/5}. \quad (100)$$

Independently from the spectral index s of the injected power law, the nonlinear synchrotron fluence at low frequencies approaches the same frequency spectral index $\alpha_{\rm NL} = 0.6$.

It is interesting to note that this behaviour of the linear and nonlinear synchrotron fluence from electrons, injected with a steep injection spectrum ($s > 2$) at low frequencies, is identical to the behaviour of the linear and nonlinear synchrotron fluence from monoenergetically injected electrons discussed in SL. Again the nonlinear fluence behaviour only occurs at frequencies much lower than the characteristic synchrotron frequencies $\nu_s \gamma_1^2$ or $K_0 U_0^{1/2} \gamma_1$, respectively, where the nonlinear fluence shows a steeper (by $\Delta\alpha = 0.1$) power-law behaviour ($\propto \nu^{-0.6}$) than the linear fluence ($\propto \nu^{-0.5}$).

9. Summary and conclusions

In powerful cosmic nonthermal radiation sources with dominant magnetic-field self generation, magnetic field generation at almost equipartition stength by relativistic plasma instabilities operates as fast as the acceleration or injection of ultra-high energy radiating electrons in these sources. Then the magnetic field strength becomes time-dependent and adjusts to the actual kinetic energy density of the radiating electrons in these sources. As a consequence the synchrotron radiation cooling of individual relativistic electrons exhibits a nonlinear behaviour because of the dependence of the magnetic energy density on the actual kinetic energy density, which itself decreases due to the time evolution of the electron number density.

For the case of instantaneous injection of power-law distributed electrons, we have solve this nonlinear kinetic equation for the intrinsic temperoral evolution of relativistic electrons. We demonstrate that the nonlinear solution for the differential electron number density depends on a new time variable $T(t)$ that is related to the intrinsic time t by a first-order nonlinear differential equation. We solved this nonlinear differential equation approximately at early, intermediate and late times to construct the $T(t)$ relation at all times after injection. The properties of the resulting approximate nonlinear electron density show significant differences from the standard linear solution for constant non-equipartition magnetic-field energy density such as the different time behaviour of the upper and lower cut-offs of the electron distribution.

By time-integration we also calculated the differential electron fluence as a function of electron energy and compared it to the linear fluence. For large spectral indices $s > 2$ of the injected power law, the nonlinear fluence exhibits a weaker break at the lower injected electron cut-off γ_1 than the linear fluence. For small spectral indices $1 < s < 2$, the nonlinear fluence shows no break at all and approaches a $\propto \gamma^{-3}$ power law at all energies below $\gamma_2/2$.

For power law injection under steady-state conditions. we demonstrated that the nonlinear and linear electron distribution functions exhibit the same dependence on the Lorentz factor of the electrons. However, under equipartition conditions, their absolute values are different. The nonlinear solution depends on the injection rate ($\propto q_0^{1/2}$) of electrons, whereas the linear solution is independent from q_0. For electron radiation processes not subject to equipartition conditions, such as inverse Compton scattering of ambient photon gases and relativistic bremsstrahlung, the energy dependences of the electron number density and the electron fluence can be used directly to infer the frequency dependence of the fluxes and fluences of the generated photons.

We also calculated the optically thin synchrotron intensity and fluence spectra taking into account the time-dependence in the nonlinear cooling case of the magnetic field strength due to the partition condition. For steep spectral indices $s > 2$, we demonstrated that fluence differences due to the nonlinear cooling from the linear cooling case only occur at small synchrotron frequencies. In this frequency range, the linear and nonlinear fluence spectral behaviours are identical to the behaviour shown by monoenergetically injected electrons. The nonlinear synchrotron fluence shows a steeper (by $\Delta\alpha = 0.1$) power-law behaviour ($\propto \nu^{-0.6}$) than the linear fluence ($\propto \nu^{-0.5}$).

Acknowledgements. We thank the referee for fruitful comments that helped to improve the manuscript. We thank Michael Zacharias for a careful checking of the manuscript. This work was partially supported by the German Ministry for Education and Research (BMBF) through Verbundforschung Astroteilchenphysik grant 05 CH5PC1/6 and the Deutsche Forschungsgemeinschaft through grant Schl 201/16-2.

References

Aharonian, F. A., Akhperjanian, A. G., Bazer-Bachi, A. R., et al. (HESS Collaboration) 2007, ApJ, 664, L71
Arbeiter, C., Pohl, M., & Schlickeiser, R. 2005, ApJ, 627, 62
Bloom, S. D., & Marscher, A. P. 1996, ApJ, 461, 79
Böttcher, M., & Chiang, J. 2002, ApJ, 581, 127
Dermer, C. D., & Schlickeiser, R. 1993, ApJ, 416, 458
Dermer, C. D., & Schlickeiser, R. 2002, ApJ, 575, 667
Felten, J. E., & Morrison, P. 1966, ApJ, 146, 686
Frail, D. A., Waxman, E., & Kulkarni, S. R. 2000, ApJ, 537, 191
Gradshteyn, I. S., & Ryzhik, I. M. 1965, Tables of Integrals, Series and Products (New York: Academic Press)
Kardashev, N. S. 1962, Sov. Astron. AJ, 6, 317
Kirk, J. G., Schneider, P., & Schlickeiser, R. 1988, ApJ, 328, 269
Maraschi, L., Ghisellini, G., & Celotti, A. 1992, ApJ, 397, L5
Melia, F., & Königl, A. 1989, ApJ, 340, 162
Meszaros, P., & Rees, M. J. 1993, ApJ, 405, 278
Meszaros, P., & Rees, M. J. 1997, ApJ, 476, 232
Paczynski, B., & Rhoads, J. E. 1993, ApJ, 418, L5
Sari, R., Piran, T., & Narayan, R. 1998, ApJ, 497, L17
Schlickeiser, R., 2008, in Proc. of workshop High Energy Phenomena in Relativistic Outflows, in press
Schlickeiser, R., & Lerche, I. 2007, A&A, 476, 1 (SL)
Sikora, M., Begelman, M. C., & Rees, M. J. 1994, ApJ 421, 153
Tavecchio, F., Maraschi, L., & Ghisellini, G. 1998, ApJ, 509, 608
Van der Horst, A. J., Kamble, A., Resmi, L., et al., 2007, A&A, 480, 35

Appendix A: Solution of electron kinetic equation for nonlinear cooling

Under equipartition conditions, the kinetic equation reads

$$\frac{\partial n}{\partial t} - A_0 \left[\int_0^\infty \mathrm{d}\gamma \gamma n \right] \frac{\partial}{\partial \gamma} (\gamma^2 n) = q_0 \gamma^{-s} H[\gamma_2 - \gamma] H[\gamma - \gamma_1] \delta(t) \quad (101)$$

with the abbreviation constant A_0. Substitute $y = A_0 t$ and set $S = \gamma^2 n$ to obtain

$$\frac{\partial S}{\partial y} - \left[\int_0^\infty \mathrm{d}\gamma S/\gamma \right] \gamma^2 \frac{\partial S}{\partial \gamma} = q_0 \gamma^{2-s} H[\gamma_2 - \gamma] H[\gamma - \gamma_1] \delta(y). \quad (102)$$

Using $x = 1/\gamma$ as independent variable, we find with $x_1 = \gamma_1^{-1}$ and $x_2 = \gamma_2^{-1}$

$$\frac{\partial S}{\partial y} + \frac{\partial S}{\partial x} \left[\int_0^\infty \mathrm{d}x\, x^{-1} S(x,y) \right] = q_0 x^{s-2} H[x - x_2] H[x_1 - x] \delta(y). \quad (103)$$

Now define T through

$$\frac{\mathrm{d}T}{\mathrm{d}y} = U(y) = \int_0^\infty \mathrm{d}x x^{-1} S(x,y) \quad (104)$$

so that

$$T(y) = \int_0^y \mathrm{d}b U(b). \quad (105)$$

Then Eq. (103) is just

$$\frac{\partial S}{\partial T} + \frac{\partial S}{\partial x} = q_0 x^{s-2} H[x - x_2] H[x_1 - x] \delta(T), \quad (106)$$

which is solved by the method of characteristics: set $x - T = \xi$ (i.e. $x = T + \xi$), implying

$$\left.\frac{\partial}{\partial T}\right|_x = \left.\frac{\partial}{\partial T}\right|_\xi + \frac{\partial}{\partial \xi}\frac{\partial \xi}{\partial T} = \left.\frac{\partial}{\partial T}\right|_\xi - \frac{\partial}{\partial \xi}; \quad \left.\frac{\partial}{\partial x}\right|_T = \frac{\partial}{\partial \xi},$$

so that Eq. (106) becomes

$$\begin{aligned} \frac{\partial S}{\partial T} &= q_0 (T + \xi)^{s-2} H[T + \xi - x_2] H[x_1 - T - \xi] \delta(T) \\ &= q_0 \xi^{s-2} H[\xi - x_2] H[x_1 - \xi] \delta(T) \end{aligned} \quad (107)$$

with the solution

$$\begin{aligned} S(x,T) &= S_h(\xi) + q_0 \xi^{s-2} H[\xi - x_2] H[x_1 - \xi] H(T) \\ &= S_h(x - T) + q_0 H[T] q_0 (x - T)^{s-2} \\ &\quad \times H[x - T - x_2] H[x_1 + T - x]. \end{aligned} \quad (108)$$

Here, $S_h(\xi)$ is any solution of $\xi = x - T$ determined by the boundary condition $S(x = 0, T) = 0$. We derive

$$S_h(-T) = -q_0 H[T] (-T)^{s-2} H[-T - x_2] H[x_1 + T]$$

or

$$S_h(z) = -q_0 H[-z] z^{s-2} H[z - x_2] H[x_1 - z]. \quad (109)$$

The solution (108) thus becomes

$$\begin{aligned} S(x,T) &= q_0 (x - T)^{s-2} H[x - T - x_2] H[x_1 + T - x] \\ &\quad \times \left(H[T] - H[T - x] \right). \end{aligned} \quad (110)$$

The final step is to calculate explicitly the time variable T as a function of y. Use Eq. (110) in Eq. (104) to write

$$\begin{aligned} \frac{\mathrm{d}T}{\mathrm{d}y} &= U = \int_0^\infty \mathrm{d}x x^{-1} S(x,y) \\ &= q_0 H[T] \int_0^\infty \mathrm{d}x x^{-1} (x - T)^{s-2} H[x - T - x_2] H[x_1 + T - x] \\ &\quad - q_0 \int_0^T \mathrm{d}x x^{-1} (x - T)^{s-2} H[x - T - x_2] H[x_1 + T - x]. \end{aligned} \quad (111)$$

For $T \geq 0$ the second integral vanishes because $x_1 + T$ and $x_2 + T$, appearing in the arguments of the Heaviside functions, are always larger than T so that

$$\begin{aligned} \frac{\mathrm{d}T}{\mathrm{d}y} &= q_0 \int_{T + x_2}^{T + x_1} \mathrm{d}x x^{-1} (x - T)^{s-2} \\ &= q_0 \int_{x_2}^{x_1} \mathrm{d}w (w + T)^{-1} w^{s-2}. \end{aligned} \quad (112)$$

Substituting $w = Tv$ then yields

$$T^{2-s} \frac{\mathrm{d}T}{\mathrm{d}y} = q_0 \int_{x_2/T}^{x_1/T} \mathrm{d}v \frac{v^{s-2}}{v + 1}, \quad (113)$$

which, for $s > 1$, can be solved in terms of hypergeometric functions (Gradstheyn & Ryzhik 1965, 3.194.5)

$$\begin{aligned} T \frac{\mathrm{d}T}{\mathrm{d}y} &= \frac{q_0}{s - 1} \left[x_1^{s-1} \, {}_2F_1 \left(1, s - 1; s; -\frac{x_1}{T} \right) \right. \\ &\quad \left. - x_2^{s-1} \, {}_2F_1 \left(1, s - 1; s; -\frac{x_2}{T} \right) \right]. \end{aligned} \quad (114)$$

For any value of s Eq. (114) yields a first order, in general nonlinear, differential equation whose solution, with the initial condition $T = 0$ for $y = 0$, then provides the relation between T and y in terms of quadratures. In the whole range of values of T or y, respectively, these integrals have to be solved numerically. Then one can use these results to write the solution (110) as a function of x and y.

For $x_1 \to \infty$ and $x_2 \to 0$ (i.e. unlimited injected power law), one can work out exactly the T to y relation as

$$T^{3-s} = q_0 (3 - s) \Gamma(2 - s) \Gamma(s - 1) y. \quad (115)$$

Appendix B: Approximate analytical methods

For a broad range of injected power laws $x_2 \ll x_1$ the integral in Eq. (113),

$$T^{2-s} \frac{\mathrm{d}T}{\mathrm{d}y} = q_0 \int_{x_2/T}^{x_1/T} \mathrm{d}v \frac{v^{s-2}}{v + 1} \quad (116)$$

can be solved approximately in the three limiting cases:

(1) small time limit $T \leq x_2 \ll x_1$;
(2) intermediate time limit $x_2 \leq T \leq x_1$;
(3) late time limit $x_2 \ll x_1 \leq T$;

respectively. We consider each case in turn.

B.1. Short time limit $T \leq x_2 \ll x_1$

In this limit we use the approximation $T \ll x_2 \ll x_1$ corresponding to

$$\frac{x_1}{T} \gg \frac{x_2}{T} \gg 1.$$

We then obtain for Eq. (116) approximately

$$T^{2-s}\frac{\mathrm{d}T}{\mathrm{d}y} \simeq q_0 \int_{x_2/T}^{x_1/T} \mathrm{d}v v^{s-3} = \frac{q_0}{s-2} T^{2-s}\left[x_1^{s-2} - x_2^{s-2}\right] \tag{117}$$

implying the linear relation

$$T(y) \simeq \frac{q_0}{s-2}\left[x_1^{s-2} - x_2^{s-2}\right] y \tag{118}$$

for short times, which behaves differently for $1 < s < 2$ and $s > 2$ respectively:

$$T(y) \simeq q_0 y \begin{cases} \frac{x_2^{s-2}}{2-s} & \text{for } 1 < s < 2 \\ \frac{x_1^{s-2}}{s-2} & \text{for } s > 2. \end{cases} \tag{119}$$

B.2. Intermediate time limit $x_2 \leq T \leq x_1$

In this limit we use the approximation $x_2 \ll T \ll x_1$ corresponding to

$$\frac{x_2}{T} \ll 1 \ll \frac{x_1}{T}.$$

We then obtain for Eq. (116) approximately

$$T^{2-s}\frac{\mathrm{d}T}{\mathrm{d}y} \simeq q_0 \left[\frac{1-(x_2/T)^{s-1}}{s-1} + \frac{(x_1/T)^{s-2}-1}{s-2}\right]. \tag{120}$$

For values $1 < s < 2$ Eq. (120) approximately reduces to

$$T^{2-s}\frac{\mathrm{d}T}{\mathrm{d}y} = \frac{1}{3-s}\frac{\mathrm{d}}{\mathrm{d}y}T^{3-s} \simeq \frac{q_0}{(2-s)(s-1)},$$

yielding

$$T(y) = \left[\frac{3-s}{(2-s)(s-1)} q_0 y + c_1\right]^{1/(3-s)}, \tag{121}$$

where the integration constant c_1 has to be determined by matching solution (121) at $T = x_2$, corresponding to $y = y_2$, to solution (119). We find

$$c_1 = -\frac{2(2-s)}{s-1}x_2^{3-s}, \quad y_2 = \frac{2-s}{q_0}x_2^{3-s} \tag{122}$$

so that

$$T(y > y_2, s < 2) \simeq \left[\frac{3-s}{(2-s)(s-1)} q_0 y - \frac{2(2-s)}{s-1}x_2^{3-s}\right]^{1/(3-s)}. \tag{123}$$

Likewise, for $s > 2$ we approximate Eq. (120) as

$$T^{2-s}\frac{\mathrm{d}T}{\mathrm{d}y} \simeq \frac{q_0}{s-2}(x_1/T)^{s-2}$$

yielding the linear relation

$$T(y) \simeq \frac{q_0}{s-2}x_1^{s-2} y + c_2 \tag{124}$$

which, apart from the integration constant c_2, is identical to the short time solution (119). The matching of the two solutions (119) and (124) at $T = x_2$ in this case then yields $c_2 = 0$, i.e.

$$T(y, s > 2) \simeq \frac{q_0}{s-2}x_1^{s-2} y. \tag{125}$$

B.3. Late time limit $T \geq x_1 > x_2$

In this limit we use the approximation $T \gg x_1 \gg x_2$ corresponding to

$$\frac{x_2}{T} \ll \frac{x_1}{T} \ll 1.$$

We then obtain for Eq. (116) approximately for all spectral index values $s > 1$

$$T^{2-s}\frac{\mathrm{d}T}{\mathrm{d}y} \simeq \frac{q_0}{s-1}T^{1-s}\left[x_1^{s-1} - x_2^{s-1}\right] \simeq \frac{q_0}{s-1}T^{1-s}x_1^{s-1} \tag{126}$$

implying the quadratic relation

$$T(y) \simeq \left[\frac{2q_0 x_1^{s-1}}{s-1} y + c_3(s)\right]^{1/2}. \tag{127}$$

The integration constant c_3 is fixed by matching the solution (127) at $T = x_1$, corresponding to $y = y_1$, to the solutions (123) and (125) for $s < 2$ and $s > 2$, respectively. For $s < 2$ we derive

$$c_3(s<2) = \frac{s-1}{3-s}x_1^2 - \frac{4(2-s)^2}{(3-s)(s-1)}x_2^{3-s}x_1^{s-1},$$

$$y_1(s<2) = \frac{(2-s)(s-1)}{(3-s)q_0}\left[x_1^{3-s} + \frac{2(2-s)}{s-1}x_2^{3-s}\right], \tag{128}$$

whereas for $s > 2$

$$c_3(s>2) = \frac{3-s}{s-1}x_1^2, \quad y_1(s>2) = \frac{s-2}{q_0}x_1^{3-s}. \tag{129}$$

B.4. Approximate solutions T(y)

Collecting terms we obtain the approximate solutions as

$$T(y, s>2) \simeq \begin{cases} \frac{q_0}{s-2}x_1^{s-2}y & \text{for } 0 \leq y \leq \frac{s-2}{q_0}x_1^{3-s} \\ \sqrt{\frac{2q_0}{s-1}x_1^{s-1}y + \frac{3-s}{s-1}x_1^2} & \text{for } y \geq \frac{s-2}{q_0}x_1^{3-s} \end{cases} \tag{130}$$

and

$$T(0 \leq y \leq y_2, s<2) \simeq \frac{q_0}{2-s}x_2^{s-2}y$$

$$T(y_2 \leq y \leq y_1, s<2) \simeq \left[\frac{3-s}{(2-s)(s-1)}q_0 y - \frac{2(2-s)}{s-1}x_2^{3-s}\right]^{1/(3-s)},$$

$$T(y \geq y_2, s<2) \simeq$$

$$\sqrt{\frac{2q_0}{s-1}x_1^{s-1}y + \frac{s-1}{3-s}x_1^2 - \frac{4(2-s)^2}{(3-s)(s-1)}x_2^{3-s}x_1^{s-1}} \tag{131}$$

with

$$y_1 = \frac{(2-s)(s-1)}{(3-s)q_0}\left[x_1^{3-s} + \frac{2(2-s)}{s-1}x_2^{3-s}\right] \tag{132}$$

and

$$y_2 = \frac{2-s}{q_0}x_2^{3-s}. \tag{133}$$

B.5. Special case s = 2

For $s = 2$ Eq. (116) holds which can be approximated as

$$\frac{1}{q_0}\frac{\mathrm{d}T}{\mathrm{d}y} = \ln\frac{T+x_1}{T+x_2} \simeq \begin{cases} \ln\frac{x_1}{x_2} & \text{for } T \le x_2 \ll x_1 \\ -\ln\frac{T}{x_1} & \text{for } x_2 \le T \le x_1 \\ \ln(1+\frac{x_1-x_2}{T}) \simeq \frac{x_1}{T} & \text{for } x_2 \ll x_1 \le T. \end{cases} \quad (134)$$

We obtain for $T \le x_2 \ll x_1$

$$T(y) \simeq q_0 y \ln\frac{x_1}{x_2}, \quad (135)$$

whereas for $x_2 \le T \le x_1$ in terms of the logarithmic integral

$$\mathrm{li}\left(\frac{T}{x_1}\right) \simeq c_4 - \frac{q_0 y}{x_1} \quad (136)$$

and for late times $T \ge x_1 \gg x_2$

$$T(y) \simeq \sqrt{2q_0 x_1 y + c_5}. \quad (137)$$

Adjusting the integration constants at the match points $T = x_2$ (corresponding to $y = y_2$) and $T = x_1$ (corresponding to $y = y_1$) we obtain

$$y_2 = \frac{x_2}{q_0}\ln\frac{x_1}{x_2},$$

$$y_1 = \frac{x_1}{q_0}\left[\frac{x_2}{x_1}\ln\frac{x_1}{x_2} + \mathrm{li}\left(\frac{x_2}{x_1}\right) - \mathrm{li}\ (1)\right] \quad (138)$$

and

$$c_4 = \mathrm{li}\left(\frac{x_2}{x_1}\right) + \frac{x_2}{x_1}\ln\frac{x_1}{x_2}, \quad c_5 = x_1^2 - 2q_0 x_1 y_1. \quad (139)$$

Collecting terms we derive

$$T(y \le y_2) \simeq q_0 y \ln\frac{x_1}{x_2}, \quad (140)$$

for $y_2 \le y \le y_1$

$$\mathrm{li}\left(\frac{T}{x_1}\right) \simeq \mathrm{li}\left(\frac{x_2}{x_1}\right) + \frac{x_2}{x_1}\ln\frac{x_1}{x_2} - \frac{q_0 y}{x_1} \quad (141)$$

and for late times

$$T(y \ge y_1) \simeq \sqrt{x_1^2 + 2q_0 x_1 (y - y_1)}. \quad (142)$$

Appendix C: Calculation of the nonlinear fluence

C.1. Steep injection power laws s > 2

With the nonlinear distribution functions (20)–(21) for large spectral indices $s > 2$ with the substitutions $z = t/t_\mathrm{L}$, $g = \gamma/\gamma_1$ and $g_2 = \gamma_2/\gamma_1$, we find

$$N_\mathrm{NL}(g, s > 2) = q_0 t_\mathrm{L} \gamma_1^{-s} g^{-s}\,[I_1(g) + I_2(g)] \quad (143)$$

with

$$I_1(g) = \int_0^1 \mathrm{d}z\,(1-gz)^{s-2} H\left[z - \left(\frac{1}{g}-1\right)\right] H\left[\left(\frac{1}{g}-\frac{1}{g_2}\right) - z\right] \quad (144)$$

and

$$I_2(g) = \int_1^\infty \mathrm{d}z\,(1-gA(z))^{s-2} \times H\left[A(z) - \left(\frac{1}{g}-1\right)\right] H\left[\left(\frac{1}{g}-\frac{1}{g_2}\right) - A(z)\right] \quad (145)$$

where

$$A(z) = \sqrt{\frac{2(s-2)}{s-1}z + \frac{3-s}{s-1}}\cdot \quad (146)$$

For the integral (145) we find

$$I_2 = \int_1^\infty \mathrm{d}z\,(1-gA(z))^{s-2} H[z - L_1(g,s)] H[M_1(g,s) - z] \quad (147)$$

with

$$L_1(g,s) = \frac{s-1}{2(s-2)}\left[\left(\frac{1}{g}-1\right)^2 - \frac{3-s}{s-1}\right],$$

$$M_1(g,s) = \frac{s-1}{2(s-2)}\left[\left(\frac{1}{g}-\frac{1}{g_2}\right)^2 - \frac{3-s}{s-1}\right] > L_1(g,s). \quad (148)$$

After inspection of the arguments of the Heaviside step functions we obtain for the contribution (144)

$$I_1(g) = \frac{1}{s-1} \times \begin{cases} 0 & \text{for } g > g_2 \\ \frac{1}{g}[1-(g/g_2)^{s-1}] & \text{for } 1 \le g \le g_2 \\ g^{s-2}[1-g_2^{1-s}] & \text{for } \frac{g_2}{1+g_2} \le g < 1 \\ \frac{1}{g}[g^{s-1} - (1-g)^{s-1}] & \text{for } \frac{1}{2} \le g < \frac{g_2}{1+g_2} \\ 0 & \text{for } g < \frac{1}{2} \end{cases} \quad (149)$$

and

$$I_2\left(g > \frac{g_2}{1+g_2}\right) = 0,$$

$$I_2\left(\frac{1}{2} < g \le \frac{g_2}{1+g_2}\right) = \frac{s-1}{s-2}\frac{1}{g^2}\left[\frac{(1-g)^{s-1} - g^{s-1}g_2^{1-s}}{s-1} - \frac{(1-g)^s - g^s g_2^{-s}}{s}\right]$$

$$I_2(g \le \frac{1}{2}) = \frac{g^{s-3}}{s-2}\left[1 - g_2^{1-s} - \frac{s-1}{s}g(1-g_2^{-s})\right]. \quad (150)$$

Collecting terms in Eq. (143), we derive

$$N_\mathrm{NL}(\gamma > \gamma_2, s > 2) = 0,$$

$$N_\mathrm{NL}(\gamma_1 < \gamma \le \gamma_2, s > 2) = \frac{q_0 t_\mathrm{L}\gamma_1}{s-1}\gamma^{-s-1}\left[1 - (\frac{\gamma}{\gamma_2})^{s-1}\right] \quad (151)$$

$$N_\mathrm{NL}(\frac{\gamma_2}{1+\gamma_2} < \gamma \le \gamma_1, s > 2) = \frac{q_0 t_\mathrm{L}\gamma_1^{2-s}}{s-1}\gamma^{-2}\left[1 - (\frac{\gamma_1}{\gamma_2})^{s-1}\right] \quad (152)$$

$$N_\mathrm{NL}\left(\frac{\gamma_1}{2} < \gamma \le \frac{\gamma_2}{1+\gamma_2}, s > 2\right) = q_0 t_\mathrm{L}\gamma^{-s} \times\left[\frac{1}{g(s-1)}[g^{s-1} - (1-g)^{s-1}] + \frac{s-1}{g^2(s-2)}\right.$$

$$\times\left[\frac{(1-g)^{s-1}-g^{s-1}g_2^{1-s}}{s-1}-\frac{(1-g)^s-g^s g_2^{-s}}{s}\right]\Bigg] \quad (153)$$

and

$$N_{\rm NL}(\gamma\le\frac{\gamma_1}{2},s>2) = \frac{q_0 t_{\rm L}\gamma_1^{3-s}}{s-2}\gamma^{-3} \times\left(1-\left(\frac{\gamma_1}{\gamma_2}\right)^{s-1}-\frac{s-1}{s}\frac{\gamma}{\gamma_1}\left[1-(\frac{\gamma_1}{\gamma_2})^s\right]\right) \simeq \frac{q_0 t_{\rm L}\gamma_1^{3-s}}{s-2}\gamma^{-3}\left(1-\frac{s-1}{s}\frac{\gamma}{\gamma_1}\right). \quad (154)$$

C.2. Flat injection power laws 1 < s < 2

Likewise for flat injection spectra we use the nonlinear distribution function (27)–(29) with the substitutions $w = t/t_{\rm M}$ and $g = \gamma/\gamma_1$ to obtain for the fluence (44)

$$N_{\rm NL}(\gamma,1<s<2) = q_0 t_{\rm M}\gamma_1^{-s}g^{-s}\left[J_1(g)+J_2(g)+J_3(g)\right] \quad (155)$$

with

$$J_1(g) = \int_0^1 {\rm d}w\left(1-\frac{g}{g_2}w\right)^{s-2} H\left[\frac{g_2}{1+g}-w\right]H\left[g-\frac{1}{1+\frac{w}{g_2}}\right]$$

$$= \int_0^1 {\rm d}w\left(1-\frac{g}{g_2}w\right)^{s-2} H\left[\frac{g_2-g}{g}-w\right]H\left[w-(\frac{g_2}{g}-g_2)\right], \quad (156)$$

$$J_2(g) = \int_1^\psi {\rm d}w\left(1-\frac{g}{g_2}D(w)\right)^{s-2} \times H\left[\frac{g_2}{1+D(w)}-g\right]H\left[g-\frac{1}{1+\frac{D(w)}{g_2}}\right]$$

$$= \int_1^\psi {\rm d}w\left(1-\frac{g}{g_2}D(w)\right)^{s-2} \times H\left[\frac{g_2-g}{g}-D(w)\right]H\left[D(w)-(\frac{g_2}{g}-g_2)\right]$$

$$= \int_1^\psi {\rm d}w\left(1-\frac{g}{g_2}D(w)\right)^{s-2} \times H[M_2(g,s)-w]H[w-L_2(g,s)] \quad (157)$$

and

$$J_3(g) = \int_\psi^\infty {\rm d}w\left(1-\frac{g}{g_2}F(w)\right)^{s-2} \times H\left[\frac{g_2}{1+F(w)}-g\right]H\left[g-\frac{1}{1+\frac{F(w)}{g_2}}\right]$$

$$= \int_\psi^\infty {\rm d}w\left(1-\frac{g}{g_2}F(w)\right)^{s-2} \times H\left[\frac{g_2-g}{g}-F(w)\right]H\left[F(w)-\left(\frac{g_2}{g}-g_2\right)\right]$$

$$= \int_\psi^\infty {\rm d}w\left(1-\frac{g}{g_2}F(w)\right)^{s-2} \times H\left[M_3(g,s)-w\right]H\left[w-L_3(g,s)\right] \quad (158)$$

with

$$\psi = t_{\rm k}/t_{\rm M} = \frac{s-1}{3-s}\left[g_2^{3-s}+\frac{2(2-s)}{s-1}\right]\simeq\frac{s-1}{3-s}g_2^{3-s}, \quad (159)$$

and

$$D(w) = \left(\frac{3-s}{s-1}w-\frac{2(2-s)}{s-1}\right)^{1/(3-s)}, \quad (160)$$

$$F(w) = \left[g_2^{s-1}\left[\frac{2(2-s)}{s-1}w-\frac{4(2-s)^2}{(3-s)(s-1)}\right] + \frac{s-1}{3-s}g_2^2\right]^{1/2} \quad (161)$$

$$M_2(g,s) = \frac{s-1}{3-s}\left(\frac{g_2-g}{g}\right)^{3-s}+\frac{2(2-s)}{3-s}, \quad (162)$$

$$L_2(g,s) = \frac{s-1}{3-s}\left(\frac{g_2}{g}-g_2\right)^{3-s}+\frac{2(2-s)}{3-s}, \quad (163)$$

$$M_3(g,s) = \frac{s-1}{2(2-s)}\left((g_2^{1-s}(\frac{g_2-g}{g})^2-\frac{s-1}{3-s}g_2^{3-s}\right) + \frac{2(2-s)}{3-s}, \quad (164)$$

$$L_3(g,s) = \frac{s-1}{2(2-s)}\left((g_2^{1-s}\left(\frac{g_2}{g}-g_2\right)^2-\frac{s-1}{3-s}g_2^{3-s}\right) + \frac{2(2-s)}{3-s}. \quad (165)$$

Inspecting again the arguments of the Heaviside step functions for the first contribution (156), we derive

$$J_1(g) = \begin{cases} 0 & \text{for } g>g_2 \\ \frac{g_2}{(s-1)g}\left[1-(g/g_2)^{s-1}\right] & \text{for } \frac{g_2}{2}\le g<g_2 \\ \frac{g_2}{(s-1)g}\left[1-\left(1-\frac{g}{g_2}\right)^{s-1}\right]\simeq 1 & \text{for } 1\le g<\frac{g_2}{2} \\ \frac{g_2}{(s-1)g}\left[g^{s-1}-(1-\frac{g}{g_2})^{s-1}\right] & \text{for } \frac{g_2}{1+g_2}\le g\le 1 \\ 0 & \text{for } g<\frac{g_2}{1+g_2} \end{cases} \quad ... \quad (166)$$

The second contribution (157) vanishes for $g < (1/2)$ and $g > (g_2/2)$ but has nonvanishing values for $(1/2) \le g \le (g_2/2)$:

$$J_2\left(\frac{g_2}{1+g_2}\le g\le\frac{g_2}{2}\right) = (s-1)\left(\frac{g_2}{g}\right)^{3-s}\int_{g/g_2}^{1-(g/g_2)}{\rm d}x\, x^{s-2}(1-x)^{2-s} \quad (167)$$

and

$$J_2(\frac{1}{2}\le g\le\frac{g_2}{1+g_2}) = (s-1)\left(\frac{g_2}{g}\right)^{3-s}\int_{1-g}^{g}{\rm d}x\, x^{s-2}(1-x)^{2-s}. \quad (168)$$

For $1 < s < 2$ and x in the indicated range of integration the power series

$$(1-x)^{2-s} = 1 + \times \sum_{k=1}^{\infty} \frac{(2-s)(1-s)\cdots(2-s-k+1)}{k!}(-1)^k x^k$$

is absolutely convergent. We then obtain for the contribution (168)

$$J_2\left(\frac{1}{2} \le g \le \frac{g_2}{1+g_2}\right) = \left(\frac{g_2}{g}\right)^{3-s}\left[g^{s-1} - (1-g)^{s-1}\right]$$

$$+(s-1)\left(\frac{g_2}{g}\right)^{3-s}\sum_{k=1}^{\infty}(-1)^k\frac{(2-s)(1-s)\cdots(2-s-k+1)}{(s-1+k)k!}$$

$$\times\left[g^{s-1+k} - (1-g)^{s-1+k}\right]. \quad (169)$$

Because $g < 1$ and for $g_2 \ll 1$ Eq. (169) is well approximated by the first leading term

$$J_2\left(\frac{1}{2} \le g \le \frac{g_2}{1+g_2}\right) \simeq \left(\frac{g_2}{g}\right)^{3-s}\left[g^{s-1} - (1-g)^{s-1}\right]. \quad (170)$$

Similarly, we find for the contribution (167)

$$J_2\left(\frac{g_2}{1+g_2} \le g \le \frac{g_2}{2}\right) = \left(\frac{g_2}{g}\right)^{3-s}\left[\left(1-\frac{g}{g_2}\right)^{s-1} - \left(\frac{g}{g_2}\right)^{s-1}\right]$$

$$+(s-1)\left(\frac{g_2}{g}\right)^{3-s}\sum_{k=1}^{\infty}(-1)^k\frac{(2-s)(1-s)\cdots(2-s-k+1)}{(s-1+k)k!}$$

$$\times\left[\left(1-\frac{g}{g_2}\right)^{s-1+k} - \left(\frac{g}{g_2}\right)^{s-1+k}\right]. \quad (171)$$

For $g \ll g_2$ we approximate Eq. (171) by its first term

$$J_2\left(\frac{g_2}{1+g_2} \le g \le \frac{g_2}{2}\right) \simeq \left(\frac{g_2}{g}\right)^{3-s}\left[\left(1-\frac{g}{g_2}\right)^{s-1} - \left(\frac{g}{g_2}\right)^{s-1}\right] \quad (172)$$

The third contribution (158) vanishes for $g > g_2/(1+g_2)$ but has nonvanishing values for lower values of g. With the substitution $x = 1-(g/g_2)F(w)$ we derive

$$J_3\left(\frac{1}{2} \le g \le \frac{g_2}{1+g_2}\right) = \int_{\psi}^{M_3} \mathrm{d}w \left(1-\frac{g}{g_2}F(w)\right)^{s-2}$$

$$= \frac{s-1}{2-s}g_2^{3-s}g^{-2}\int_{g/g_2}^{1-g}\mathrm{d}x\,(1-x)x^{s-2}$$

$$= \frac{s-1}{2-s}g_2^{3-s}g^{-2}$$

$$\times\left[\frac{(1-g)^{s-1}-(g/g_2)^{s-1}}{s-1} - \frac{(1-g)^s-(g/g_2)^s}{s}\right] \quad (173)$$

and

$$J_3\left(g \le \frac{1}{2}\right) = \int_{L_3}^{M_3}\mathrm{d}w\left(1-\frac{g}{g_2}F(w)\right)^{s-2}$$

$$= \frac{s-1}{2-s}g_2^{3-s}g^{-2}\int_{g/g_2}^{g}\mathrm{d}x\,(1-x)x^{s-2}$$

$$= \frac{s-1}{2-s}g_2^{3-s}g^{-2}\left[\frac{g^{s-1}-(g/g_2)^{s-1}}{s-1} - \frac{g^s-(g/g_2)^s}{s}\right] \quad (174)$$

Because $g < 1$ and $g_2 \gg 1$ we approximate (173) and (174) as

$$J_3\left(\frac{1}{2} \le g \le \frac{g_2}{1+g_2}\right) \simeq \frac{g_2^{3-s}}{(2-s)s}g^{-2}(1-g)^{s-1}[1+(s-1)g] \quad (175)$$

and

$$J_3\left(g \le \frac{1}{2}\right) \simeq \frac{g_2^{3-s}}{2-s}g^{s-3}\left[1-\frac{s-1}{s}g\right]. \quad (176)$$

Collecting terms yields for the fluence (155)

$$N_{\rm NL}(g, 1<s<2) = q_0 t_{\rm M}\gamma_1^{-s}J(g) \quad (177)$$

with

$$\begin{aligned} J(g>g_2) &= 0, \\ J\left(\frac{g_2}{2} \le g \le g_2\right) &= \frac{g_2}{s-1}g^{-(s+1)}\left[1-(g/g_2)^{s-1}\right], \quad (178) \\ J\left(1 \le g \le \frac{g_2}{2}\right) &= g_2 g^{-(s+1)}\left[\frac{1-(1-\frac{g}{g_2})^{s-1}]}{s-1}\right. \\ &\quad \left. + (g_2/g)^{2-s}\left(\left(1-\frac{g}{g_2}\right)^{s-1} - \left(\frac{g}{g_2}\right)^{s-1}\right)\right] \\ &\simeq g_2^{3-s}g^{-3}\left((1-\frac{g}{g_2})^{s-1} - \left(\frac{g}{g_2}\right)^{s-1}\right) \quad (179) \end{aligned}$$

and

$$J\left(g \le \frac{1}{2}\right) \simeq \frac{g_2^{3-s}}{2-s}g^{-3}\left[1-\frac{s-1}{s}g\right]. \quad (180)$$